Research Square

Preprints are preliminary reports that have not undergone peer review.
They should not be considered conclusive, used to inform clinical practice,
or referenced by the media as validated information.

Tectonic-petrological model of the multistage origin of eclogites of the Maksyutov complex (Southern Urals)

Valentin Fedkin

fedkin@chgnet.ru

Korzhinskii Institute of Experimental Mineralogy Russian Academy of Sciences

Andrey Shchipansky

Geological Institute, Russian Academy of Sciences

Research Article

Keywords: Maksyutov complex, eclogite, subduction initiation, ultra-high-pressure metamorphism, tectonic-petrological model, geodynamics

Posted Date: August 27th, 2026

DOI: https://doi.org/10.21203/rs.3.rs-10710707/v1

License: This work is licensed under a Creative Commons Attribution 4.0 International License.
Read Full License

Additional Declarations: The authors declare no competing interests.

Tectonic-petrological model of the multistage origin of eclogites of the Maksyutov complex (Southern Urals)

Valentin Fedkin*[1], Andrey Shchipansky[2]

✉ **Valentin Fedkin**

vfedkin@iem.ac.ru

[1] D.S. Korzhinsky Institute of Experimental Mineralogy, Russian Academy of Sciences 142432, Chernogolovka, Moscow Region, 4, Ac. Osipyan Str.

[2] Geological Institute, Russian Academy of Sciences 119017 Moscow, Pyzhevsky Per 7

Abstract

The Maksyutov eclogite-blueschist complex in the Southern Urals (MC) is well known as a classic high- to ultrahigh-pressure (HP-UHP) crustal eclogite complex. Extensive geologic, petrological, and geochemical data collected over nearly 60 years of study of the MC, allow us to construct a model for the formation and evolution of subduction structures in crustal collision zones based on modern geodynamic concepts. Our testing of the latest geodynamic concept, the "Subduction Initiation Rule" (SIR), demonstrated that the key features and criteria for subduction initiation in this terrane are sufficiently well represented and clearly observed. New high-precision analytical data on the chemical composition of rocks and minerals in the complex, obtained from a specially selected sample collection, made it possible to use a modern geodynamic classification of oceanic basalts and establish a number of features and phenomena, as well as the structure and evolution of the Maksyutov terrane. Based on a wide range of chemical elements (major, trace, and rare earth, including HFSE and LILE), the proportion of the subduction component for this complex was

estimated for the first time from 1 to 4%, and the pressure range (1.5–3.5 GPa) of mantle-crust interaction and magma generation in the mantle plume and depleted mantle was determined. An unusual cyclical recurrent-pulsational nature of the metamorphism of MC rocks was established, determining the state of the reference ultrahigh-pressure minerals: diamond and coesite. It was shown that these phases were trapped and emplaced into the MC by the mantle plume, rather than formed in situ as a result of progressive metamorphism. On this basis, the rating of the Maksyutov terrane as an ultra-high-pressure complex is called into question, which entails a significant revision of its geodynamic history.

Keywords Maksyutov complex • eclogite • subduction initiation • ultra-high-pressure metamorphism • tectonic-petrological model • geodynamics

Introduction

The Maksyutov eclogite-blueschist complex in the Southern Urals is well known as a high-pressure/ultra-high-pressure (HP-UHP) complex and is widely popular among researchers due to the presence of diamond and coesite in its rocks. The long history of studying this terrane and the large body of factual material accumulated over nearly 60 years of research create unique opportunities for identifying general principles of crustal eclogite formation and developing a model for their tectonic-petrological history. In addition to general works on the structure and development of the Maksyutov eclogite-blueschist complex (Valizer and Lennykh 1988; Lennykh et al. 1995; Dobretsov et al. 1996; Lennykh and Valizer 1999; Leech and Ernst 2000; Brown et al. 2006; Beane and Leech 2007; Puchkov 2010), targeted studies on petrology, geochemistry, geochronology, tectonics and geodynamics were carried out within this terrane. All reports of the presence of high-pressure minerals (diamond and coesite) in the rocks of the Maksyutovsky complex have been

carefully studied, but each time these observations have been considered as evidence of high-temperature metamorphism (Chesnokov and Popov 1965; Leach and Ernst 1998; Korsakov et al. 2019), which created a persistent opinion about UHP conditions of terrane formation. Recently, much attention has been paid to the origin of high-temperature and high-pressure ultramafic inclusions in the eclogite-schist sequence of the complex, their age and PT formation parameters (Valizer et al. 2011, 2013a, 2013b; Rusin et al. 2021; Perchuk et al. 2024). At the same time, ideas are developing about the unusual nature of the metamorphism of the terrane rocks, the chemical heterogeneity of the rock-forming minerals and the relationship of these features with the geodynamic history of the region (Beane and Leech 2007; Kovalev et al. 2015; Valizer et al. 2015; Fedkin 2020; Fedkin et al. 2021).

The idea of developing a tectonic-petrological model for the origin and evolution of crustal eclogites arose from the new geodynamic concept of the "Subduction Initiation Rule" (Whattam and Stern 2011; Whattam 2023), which initially set us the task of testing and approximating the SIR using the Maksyutov complex as an example. The implementation of this idea could not be carried out without taking into account the geodynamic classification of oceanic basalts (Pearce 2008), which linked geodynamic issues with the geochemical composition of the rocks of the complex. The classification of oceanic basalts by Pearce (2008) allows us to assess the significance and role of large structural fragments of the Earth's crust as participants in the subduction process, determine their magma-generating role as a source of source material, and evaluate the mantle-crust interaction in this process. To address these challenges, it was necessary to perform highly accurate analyses of the complex's eclogite rocks for a wide range of chemical elements, including trace, and rare-earth elements, including HFSE and LILE. To this end, the most informative and well-studied areas of the MC were selected, within which a control collection of representative HP-UHP mafic rocks (eclogites, Grt-Cpx, and Grt-Gln schists) was selected for a targeted study of their chemical composition and physicochemical formation parameters. New geochemical and petrological data provided the quantitative basis for solving the complex problem of developing a tectonic-

79 petrological model for crustal eclogites. The results of these petrological studies have been partially
80 published previously (Fedkin et al. 2017; Fedkin 2020). XRF and ICP MS data for the bulk rock
81 composition are presented in Supplementary Tables 1 and 2. Microprobe analyses of minerals from
82 these same samples were previously used to study the chemical heterogeneity of rock-forming
83 minerals and the metamorphic features of the complex (Fedkin 2021). These data and the results of
84 these studies are also taken into account in this paper.

85 The solution to the problem of developing a tectonic-petrological model for the Maksyutov
86 complex was initially based on the Subduction Initiation Rule (SIR) concept (Whattam and Stern
87 2011; Whattam 2023). This recent concept considers the subduction process in fore-arc basins in
88 connection with the formation of ophiolite complexes and the development of a chemostratigraphic
89 diagnostic magmatic sequence of specific compositional changes in basalts in the ophiolite part of
90 the complex based on the content of rare and trace elements, including HFSE and LILE. Are the
91 identified patterns common to eclogite-glaucophane schist complexes, or are they random,
92 reflecting only the specific characteristics of a particular region? The answer to this question
93 determined the initial goal of this study. However, a detailed examination of the task at hand
94 revealed the broader potential of the collected material for developing a tectonic-petrological model
95 for the origin and development of crustal eclogites.

96 The Maksyutov complex is considered as a unique object for testing and adapting the SIR
97 concept as a general model for the formation and development of crustal subduction of eclogite
98 complexes. Key criteria and features of the Subduction Initiation Rule in the MC are presented
99 fairly fully and are clearly implemented. The formation time of the high-temperature/high-pressure
100 (HT/HP) subduction channel of the MC subduction and its metamorphism coincides with the
101 emergence of the Magnitogorsk intraoceanic island arc in the Early Devonian (Brown et al. 2006;
102 Puchkov, 2010). Thus, the temporal combination of the initial stages of the SIR is realized. The two
103 main structural-lithological units of the terrane – the lower eclogite-schist and the upper ophiolite –
104 are combined into a single structural-lithological package of the complex (Lennykh et al. 1995),

which confirms the spatial combination of eclogites and ophiolites. Geochemical data on major, trace, and minor elements of the complex generally establish a chemostratigraphic diagnostic magmatic sequence for the composition of metabasic rocks in the ophiolitic part of the MC, although some aspects of this rule require clarification. The only conduit for HT/HP subduction and exhumation of the complex is the MC itself (Valizer and Lennykh 1988; Dobretsov et al. 1996; Puchkov 2010).

However, the geochemical, petrological, and geodynamic features of the complex complicate the interpretation of the Subduction Initiation Rule as a general framework for the origin and development of subduction. Even the "unique conditions" of the MC leave a number of controversial issues, most likely related to the tectonics of the orogen rather than the general criteria of these rules. The most controversial and interesting of these are considered and discussed below. They do not address the essence of the subduction initiation problem, but supplement the obtained patterns with characteristic features of the complex under study.

Geological Position of the Maksyutov complex

The Maksyutov eclogite-glaucophane schist complex is located in the southeastern part of the western slope of the Southern Urals in the Sakmara River basin and represents a mélange belt of metamorphic rocks, tectonically sandwiched between the predominantly Ediacaran sequence of metaterrigenous rocks of the Suvanyak Formation to the west and the mélange of the Main Ural Fault (MUF) zone to the east (Fig. 1). The complex, approximately 15-20 km wide, outcrops as a narrow band extending north-south for approximately 200 km (Lennykh et al., 1995; Braun et al., 1998). Its structural thickness is ~5-10 km (Dobretsov,1974; Hetzel et al.,1998; Hetzel 1999). The contacts with adjacent geological formations are tectonic and steeply inclined to the east. The

complex is bounded on the west by the Lower Paleozoic formations of the Sakmara zone and the Suvanyak complex of the East European platform (Zonenshain et al. 1984, 1990; Zakharov 1991; Puchkov 1993; Matte 1995; Scarrow et al. 2002). From the east, the tectonic boundary of the complex is defined by the Main Ural Fault, where it adjoins the Lower Paleozoic metabasalts of the Kempirsay Belt, an integral part of the Magnitogorsk island arc (Senger et al. 1993; Berzin et al. 1996).

Petrographic sketches

Within the complex, two structural-compositional (lithological-tectonic) units are traditionally distinguished, forming a composite plate of high and ultrahigh pressure (Valizer and Lennykh 1988, Lennykh et al. 1995; Dobretsov et al. 1996), although genetic representations of these "suites" seem redundant.

The lower "subcontinental" eclogite-glaucophane schist unit #1 is a polymetamorphosed eclogite-blueschist lithological association. It includes mafic glaucophane and feldspar-mica schists, interbedded with quartzites. This unit contains numerous eclogite lenses, boudins, and interbeds, garnet-pyroxene, and less abundant olivine-enstatite rocks. Unit #1 underwent high- and ultrahigh-pressure metamorphism, which was later overlain by glaucophane-greenschist facies associations at lower pressures.

The upper, "ophiolite-like" unit #2 consists of oceanic crustal rocks and includes an underlying basal metaophiolite. It consists of oceanic crustal rocks and associated overlying graphitic schists and metagraywackes formed during the pre-metamorphic stage of Ordovician-Silurian seafloor spreading. This upper block also includes irregular bodies and lenses of serpentinite and marble, as well as metabasaltic rocks with lawsonite eclogites and metaultramafics. Block No. 2 underwent metamorphism to blueschist facies and then to greenschist facies.

The intermediate Yumaguzinsky unit of metasedimentary rocks of unknown origin is part of the lower series. It consists of subducted distal turbidites and includes quartzites and mica schists with rare inclusions of garnet-pyroxene rocks and eclogites. However, the Paleozoic origin of this unit remains unclear. For constructing a tectonic-petrological model (TPM) of the Maksyutov complex, the lower structural unit is of greatest petrological interest. It is dominated by metasedimentary rocks with boudins and tectonic blocks of eclogites, less commonly metaultramafics, which, along with Ol-En, Qz-Jd, and Low associations, determine the culminating progressive metamorphic P-T conditions. Ophiolite block #2, among rocks of serpentinite mélange, lawsonite metarodingites, and gabbro amphibolites, also contains blocks of ultramafic composition, metabasaltic blueschists, and metasedimentary quartz-jadeite rocks, exhibiting HP-UHP formation parameters.

The protolith is Precambrian in age; the earliest Zr dates, likely from ancient provenances, span the range from 1.1-1.4 to 2.35-2.84 billion years (Valizer et al. 2011). There are two points of view regarding the formation of the Maksyutov complex. According to one, the Maksyutov complex eclogites formed during intense UHP metamorphism 550-600 million years ago (Valizer and Lennykh 1988). The final stage of HP metamorphism (320-385 million years ago) occurred simultaneously with the metamorphism of the ophiolite portion of the complex (Dobretsov 1974). According to the second point of view, the eclogites formed from Middle Devonian oceanic basalts (370-380 million years ago). Some researchers see this as a two-stage development of the terrane (Dobretsov 1996; Shatsky et al. 1997; Valizer et al. 2011). However, a consensus of sorts has recently emerged among researchers on this issue: ~390 Ma.

The maximum parameters of eclogite metamorphism, judging by the findings of diamond and coesite microinclusions in the rocks of the complex (Bostick et al. 2003; Rusin et al. 2021), were estimated at the limit of the PT region of their stability: at temperatures up to 650-700 °C and pressures up to 2.8-3.2 GPa (Lennykh and Valizer 1999; Dobretsov et al. 1996). However, the extremely rare occurrence of these phases in MC rocks and the not very high level of progressive

metamorphism ending at a depth of ~90-120 km under conditions of P < 2.5-3.2 GPa and T < 740-790 °C (Lennykh et al. 1995; Leech and Ernst 2000; Brown et al. 2006; Beane and Leech 2007; Valizer et al. 2013b) do not allow us to say with certainty that ultra-high pressure conditions were realized during the formation of MC. More detailed information on the conditions of metamorphism and the formation of UHP rocks and minerals is given below in the following sections of the article.

Methods

For constructing a tectonic-petrological model (TPM) of the Maksyutov complex, the lower structural unit is of greatest petrological interest. It is dominated by metasedimentary rocks with boudins and tectonic blocks of eclogites, as well as metaultramafic rocks, which, along with Ol-En, Qz-Jd, and Low associations, determine the culminating progressive metamorphic P-T conditions. In ophiolite block No. 2, among the rocks of serpentinite mélange, lawsonite metarodingites and gabbro-amphibolites, there are also blocks of rocks of ultramafic composition, metabasaltic blue schists and metasedimentary quartz-jadeite rocks with fairly high formation parameters.

For studying the high-pressure associations of the complex, the most representative and easily accessible area is the area from the village of Shubino to the former village of Karayanovo, stretching approximately 35 km from north to south. For this reason, it is also the most thoroughly studied area in all respects. We selected this area as the reference for studying the high-pressure formations of the Maksyutov complex (Fig. 2). Several intermediate points between them, near the villages of Novosimbirka, Antingan, and Ivanovka, were also studied to compare the conditions of eclogite formation in different areas of the complex. Supplementary Materials 1 (SM-1) presents a detailed map of the surveyed areas and their geological structure. Eighteen representative samples of high-temperature mafic rocks from the lower structural-material block of the complex were selected as a control series. The list and mineral composition of these samples are given in Supplementary Materials 2 (SM-2), Table 1. Table 2 in SM-2 represents the P-T conditions of

formation of each sample. The bulk chemical composition of the rocks was analyzed for rock-forming, trace, and rare earth elements using X-ray fluorescence (XRF) and inductively coupled plasma mass spectrometry (ICP-MS). One sample (nos. 158 and 158R) was analyzed twice as two independent analyses, confirming the high reproducibility of the analytical results. XRF and ICP-MS data for the rocks, as well as the normative mineral compositions, are presented in Supplementary Materials 3 (SM-3), Tables 1 and 2, respectively.

The chemical composition (XRF and ICP MS analyses) is presented in SM-2: Table 1. General composition of rocks analyzed by XRF, and Table 2. Composition of trace, microelements, and rare earth elements. Mineral relationships, petrographic descriptions, and thin-section micrographs of the most typical samples are presented in Supplementary Materials 4 (SM-4).

The traditional petrological approach of cation-exchange thermobarometry (Perchuk et al. 1983) was used to study the physicochemical conditions of metamorphism and transformation of eclogite associations. The chemical composition of minerals, their heterogeneity, and zoning were studied in the same series of selected samples using electron probe X-ray analysis (EPXRA). Primary attention was paid to the complex multidirectional zoning of garnet, the most informative mineral and the one most sensitive to changes in metamorphic parameters. Both large porphyroblastic grains of contacting grains and small newly formed crystals in the groundmass, grains with direct and reverse zoning, and various variants of inversion zoning were studied. Examples of such zoning have been described in detail in previous studies (Fedkin et al. 2017, 2021; Fedkin 2020, 2024) and are also shown in microprobe micrographs in Supplementary Materials 5.

Microprobe analysis was performed using a Tescan Vega II XMU scanning electron microscope (Tescan, Czech Republic) equipped with an INCA Energy 450 X-ray microanalysis system with an energy-dispersive X-ray spectrometer (INCAx-sight) (Oxford Instruments, England). The range of elements analyzed ranged from Be to U. Analysis conditions included an accelerating voltage of 20 kV, an absorbed electron current on Co of 0.3 nA, and an analysis time of

70 s. The analytical lines and standards of the Institute of Experimental Mineralogy of the Russian Academy of Sciences applicable to X-ray microprobe analysis were used: Na - albite, K - orthoclase, Mg - MgO, Ca - wollastonite, Si - SiO2, Al - Al2O3, Fe, Mn, and Ti - the corresponding pure elements. The analytical error did not exceed 2 rel. %.

To assess the P-T conditions of the formation of eclogites and other Grt-Cpx equilibria, a Powell (1985) mineralogical geothermometer and an improved Perchuk (1992) geobarometer were used. Primary attention was paid to relative changes in temperature and pressure during the crystallization of zoned garnet grains, at contacts and in inclusions with other minerals, which allows us to assess the nature of evolutionary PT trends in rock crystallization during the formation of the complex. P-T parameters calculated using a Grt-Cpx geothermometer and a Pl-Cpx-Qz geobarometer generally correspond well to petrographic and geological data. However, plagioclase, necessary for pressure estimation, is preserved only during the final regressive stages of metamorphism and typically has a substantially albite composition—no more than 2-3 mol % anorthite. Its use for pressure estimation in equilibrium with progressively zoned garnet is therefore conditional, although these data highlight the temperature trend. In high-pressure associations beyond the Ab-Jd-Qz equilibrium, matrix plagioclase grains sometimes have to be used to estimate pressure, although the data obtained in this way provide only approximate forced values of quasi-equilibrium pressure.

Results

A control collection of representative samples of high-temperature rocks from the Maksyutovsky Complex, specifically collected to develop a tectonic-petrological model for the formation of Maksyutov ccomplex eclogites, was studied for petrography, bulk chemistry, trace element geochemistry, and chemical heterogeneity of the rock-forming minerals. The results of these studies

have been partially published in the authors' previous works **(Fedkin, 2020, 2024; Fedkin et al. 2021)** and in **Supplementary Materials 3-5.** Eighteen samples of garnet-bearing mafic rocks from the lower block of the Maksyutov complex were analyzed for a wide range of chemical elements, including rock-forming elements, trace elements, and rare earth elements, including the HFSE and LILE groups. The general composition of the rocks and the composition of zoned grains of coexisting phases for mineralogical thermobarometry were determined on the same control samples using electron probe X-ray analysis (microprobe analysis). The most representative microprobe photographs are presented in SM-5.

Geochemistry of major, trace, and rare earth elements in the MC

New geochemical data on the composition of representative samples of high-pressure rocks in the MC (Fedkin et al. 2021) are quite conventional. They highlight the main features of the SIR, characterize the subduction environment, and create certain prerequisites for its occurrence and development. A wide range of compositions of the eclogites of the complex is noted for **the main rock-forming elements.** All samples fall into the low-potassium basalt region, and only a few of them correspond to andesite-basalts with a range of SiO_2 contents: from 41.8 to 61.12 wt%. The rocks also show a wide range of contents of TiO_2 (0.8-4.7 wt%), Al_2O_3 (12.0-16.2 wt%), FeO* (6.3-17.1 wt%), MgO (5.3-9.0 wt%), CaO (5.4-12.4 wt%), Na_2O (1.9-6.8 wt%), K_2O (0.02-1.0 wt%) and P_2O_5 (0.1-0.8 wt%) (Supplementary materials 3, Table 1). Previously published data on the MC rocks as a whole (Volkova et al. 2004; Beane and Sorensen 2007) only expand the compositional range of the Maksyutov eclogites and blueschists, but do not change the fractionation trend, reflecting the compositional transition from basalts to andesites. Trends in crystallization fractionation (a decrease in the Fe-Mg component and an increase in Na_2O reflect the compositional transition from basalts to andesites. The alkali-silica ratio demonstrates typical differentiation trends from magmatic to metamorphic protolith of high-pressure rocks of the complex (Le Bas and

Streckeisen 1991). In AFM coordinates (Fig. 3), the MC eclogites form a single trend of basalt evolution from tholeiitic to calc-alkaline series, including both depleted and enriched compositions.

Similar ratios of tholeiitic and calc-alkaline basalts can arise directly during subduction initiation. For example, in the Paleogene ophiolites of New Zealand, which are composed primarily of tholeiitic basalt, the proportion of calc-alkaline lavas is ~25% (Whattam 2023). An important reason for this transformation could have been the influx of fluid and a change in the oxygen regime in young subduction structures during the SIR process. The compositional changes of MC eclogites and the very similar ratios of basalt compositional changes in modern and mature subduction systems confirm the evolutionary trend of the initial mantle melts as one of the important features of the "Subduction Initiation Rules." On the other hand, the alkali-silica ratio in the Maksyutov eclogites demonstrates typical differentiation trends of metamorphism of the protolith of high-pressure rocks (Le Bas and Streckeisen 1991), which indicates the superposition of metamorphic processes on the initial mantle melts in the history of the complex's development.

It is known that highly incompatible (HFSE) and rare earth (REE) elements are relatively immobile during high-pressure metamorphism, while large lithophile elements (LILE) exhibit significant mobility (Creaser et al. 1999). Therefore, **incompatible elements are the best indicators of the protoliths** of mafic rocks in the eclogite complex. The compositions of the 18 analyzed MC eclogite samples in terms of incompatible element content generally vary around the average MORB composition, deviating slightly in either direction—either toward the more depleted N-MORB rocks or toward the enriched OIB fore-arc basalts (Fig. 4). Moreover, the ratio of depleted to enriched compositions of the studied samples across all surveyed areas of the complex remains at a 1:2 ratio, indicating a uniform pattern of changes in subduction conditions.

Geochemistry of trace and rare earth elements in rocks of the Maksyutov complex

Figure 4 illustrates **the geochemical characteristics of rare earth and trace elements** in rocks of the Maksyutov complex. Discrimination diagrams for the 18 analyzed mafic rocks show that eclogite and blueschist compositions are widely represented in all three profiles. This allows us to distinguish between oceanic, island arc, and continental basalts in different tectonic settings. Eclogites and glaucophane schists from all sites (Shubino, Antingan, Novosimbirka, Karayanova, and Ivanovka; Fig. 2) exhibit similar element distributions. This distribution could be due to either the significant compositional variation of the protoliths from a wide range of tectonic environments or the contrasting nature of Na-metasomatism accompanying different stages of recrystallization of these rocks (e.g., ocean floor metasomatism, prograde and retrograde metamorphism during subduction and/or exhumation). However, no consistent change in the geochemical spectrum of elements is observed across different sections of the complex. This suggests that the heterogeneous compositions of the mafic eclogites were likely typical for this entire region of the Maksyutov complex.

The rare earth element distribution spectra of MC HP rocks, normalized to chondrite (Fig. 5), show the same diversity as for trace elements. Their composition is not significantly different from that of N- and E-type MORB basalts. Moderate enrichment in light rare earth elements (LREE) suggests partial melting of oceanic metabasalts in the subduction zone or their metasomatic alteration. *The normative calculations* presented in Supplementary Materials 3 Table 1 also demonstrate the chemical diversity of the analyzed eclogites and glaucophane schists of MC. Five samples (158, 207, 213, 289, and 230/231) are Ne-normative, and four samples (161, 163, 185, and 219) are Qz-normative. Two samples stand out for their anomalous composition. Sample 219 from the Karayanovo area contains almost 4% Q. According to the relatively high normative Q value (3.91%), as well as Mg# (Mg/(Mg + Fe*) 0.52 and Ca# (Ca/(Ca + Na) 0.33 values, the major element proportions of this rock clearly indicate an andesitic composition. Sample 235/236 has the highest Mg# value, 0.65, and relatively high Ca# value, 0.57, suggesting a cumulative origin of mafic magma. The remaining 16 rocks studied include silica-deficient rocks. Their chemical

compositions as a whole do not show any noticeable fractionation trend with respect to the presence of Ne or Q. Thus, normative variations in these mafic igneous rocks are likely a function of heterogeneous mantle-source lithologies and/or subsequent metasomatism in contrasting plate tectonic settings. Based on the composition of the main elements, we cannot unambiguously identify a single igneous precursor of the garnet-bearing mafic rocks of the MC. Clearly, the protoliths comprising this mafic complex either formed in different areas of plate tectonics or subsequently underwent varying degrees of chemical exchange in an open system.

Composition of rock-forming minerals

The composition of rock-forming minerals has been previously studied during P-T studies of metamorphism. The results of these studies, as well as analyses of garnet, clinopyroxene, and plagioclase, are presented in separate publications (Fedkin et al. 2017; Fedkin 2020). Here, we provide only brief information on these phases, which determine the equilibrium conditions of their crystallization in the Grt + Cpx + Pl + Qz paragenesis.

Garnet is present in almost all studied samples as large porphyroblastic segregations and smaller, often idiomorphic, crystals within the rock groundmass. Garnet exhibits chemical and morphological heterogeneity throughout its volume. Chemical zoning of large garnet grains in most studied samples reveals progressive, retrograde, and sometimes inverted P-T trends under the crystallization conditions of its assemblages. Examples of such zoning are shown in micrographs from microprobe surveys in Supplementary Materials 5. In some cases, traces of these processes are contained within a single sample or, more interestingly, even within a single garnet grain.

Clinopyroxene, in the form of small (0.1-0.4 mm) short-prismatic crystals, is present in the groundmass of the rock along with glaucophane, epidote, chlorite, muscovite, and quartz. Pyroxene inclusions in garnet are compositionally identical to the matrix grains, which are also used to determine the P-T parameters of the Grt-Cpx-Ab-Qz equilibrium. The composition of

clinopyroxene in MC rocks is close to omphacite, varying in individual samples in the range of X_{Jd} ~ 0.2-0.40, and in a single grain, the mole fraction of the jadeite component does not exceed 0.30-0.35. Extensive observations of the phase compositions in the Grt-Cpx pair have shown that P-T trends in the formation of eclogite associations are primarily determined by the chemical zoning of garnet, with omphacite behaving completely inertly.

Plagioclase, necessary for estimating pressure in equilibrium with garnet, clinopyroxene, and quartz, is found only in relatively low-temperature rocks of the complex that have undergone retrograde secondary alteration. Plagioclase inclusions in large garnet grains significantly facilitate the interpretation of metamorphic conditions during rock formation. The composition of plagioclase varies from almost pure albite to An_{5-7}. Microprobe compositional estimates underestimate the sodium content of the mineral due to sodium loss during the study, and the actual measured plagioclase composition does not exceed three units of anorthite component. This error naturally underestimates the equilibrium pressure in the Grt-Cpx-Pl-Qz association by 0.1-0.2 GPa. However, when comparing relative pressures, such deviations in the composition of plagioclase are not of fundamental importance.

Discussion

Geochemical criteria for subduction initiation

The results of geochemical studies of a control series of high-pressure MC rocks define the main requirements for subduction initiation (Whattam and Stern 2011). These are primarily the basaltic (not gabbroic) composition of the initial protolith melt and its metamorphic origin, as evidenced by the absence of Eu and Sr anomalies in the REE spider diagrams (Fig. 5). Secondly, the composition of the presumed parent basalts forms a continuous evolutionary trend from tholeiitic to calc-alkaline

(Fig. 3a). This sequence of compositional evolution of the basalt series is an indication of a change in their mantle sources from N-MORB to OIB, respectively. The listed data form the basis for the formation of a chemostratigraphic sequence of the metabasites of the ophiolite unit of the complex and are treated as independent and necessary within the concept of the Subduction Initiation Rule. However, only two indicators can be directly related to the SIR: the wide range of eclogite compositions (Fig. 3) and the diversity of sources of their parent material (Fig. 4). For the proposed concept these criteria are of minor importance, but certain conditions are necessary for their fulfillment. The formation of high-pressure rocks of the MC requires at least a three-component source of parent material: enriched OIB mantle, depleted N-MORB and E-MORB mantle, and some contribution from subduction (crustal contamination). The accumulation of such diverse material in a single complex requires a long time, which raises the question of the time of the onset of subduction and the duration of the existence of the Maksyutov complex, quite possibly from the Early Paleozoic to the Devonian inclusive.

The question of the origin and age of the Maksyutov complex is not new. It was previously raised for various reasons: in connection with early (Paleoproterozoic) estimates of the age of the MC rocks protolith (Dobretsov 1974; Dobretsov et al. 1996) and the age of high-pressure ultramafic inclusions (Valizer et al. 2011); in connection with the finds of conodonts in Ordovician sediments and the model of a two-stage development of the complex (Shatsky et al. 1997); as well as in connection with suprasubduction changes in the oceanic lithosphere in Ordovician time (Ryazantsev et al. 2008) and the age of the Ural oceanic basin. In light of the SIR concept, this entire chain of questions becomes more acute and requires a solution, complementing and clarifying the general model of the complex's development.

A key feature of the composition of high-pressure rocks of the MS is their enrichment in niobium. This issue is fundamental, since so-called Nb-enriched basalts (NEB) are a sensitive indicator of ocean ridge subduction. The relationship of NEB samples (usually depleted) with the oceanic (N-MORB and E-MORB) substrate is clearly visible in Pearce diagrams (Pearce, 2008)

(Figs. 6, 7). This geochemical indicator raises a number of geodynamic questions (a unique symbiosis of geochemical and geodynamic factors) both in relation to subduction processes and to problems in the historical development of the complex.

Firstly, this suggests a revision of the polarity of the MC subduction in the Guberlin Island Arc region from east to west (Ryazantsev et al. 2008; Ryazantsev and Tolmacheva 2016), which fundamentally alters the course of the entire orogen's evolution. The main event in the geodynamic evolution of the MC is the subduction of Paleo-Asian oceanic crust beneath the continent, not the subduction of the East European Craton margin. However, the eastward dip of continental subduction beneath the Devonian Magnitogorsk Island Arc (Puchkov 2010) is not disputed in these studies, and this idea remains only a special case within the overall complex.

Secondly, naturally, this question is related to the origin of the Ural Oceanic Basin. Was it part of the Central Asian paleoocean, or did it form at the beginning of the Paleozoic? The duration of the Ural Ocean's existence (100 or more than 100 million years) determines not only the role and degree of participation of the subduction component in the MC rocks but also the duration of the entire complex's existence.

The contribution of the subduction component to high-pressure MC rocks is determined by their composition of trace and trace elements, according to model calculations (Pearce 2008). Nb-enriched basalts are a good indicator of the participation of the subduction component in the SIR. Taking into account the control compositions of the complex's rocks (Fedkin et al. 2021), both depleted and enriched, this contribution ranges from 1.0 to 4.0% (Fig. 6). Not a very high percentage, but even such participation of the crustal component in the composition of MC rocks according to the Nb/Thn parameter (up to 2.38-7.11 in the area of the village of Shubino (Fedkin et al. 2021) exceeds the strange indicators of young subduction structures in the Northland segment of the southwestern Pacific Ocean by almost three times - 1.54 (Whattam 2023).

It remains unclear whether this component was present in the MC rocks at the onset of the subduction process or whether it is associated with suprasubduction changes in the oceanic

lithosphere during the formation of the Early Devonian P-MORB ridge in the Southern Urals in Ordovician time (Ryazantsev et al. 2008). However, calculations clearly indicate its participation in subduction, similar to that noted in the Permian Yukon-Tanana terrane in the northern Canadian Cordillera (Colpron et al. 2025). The presence of boninites in ophiolites in the western Magnitogorsk zone (Kuzmin and Kabanova 1991) emphasizes the active participation of this component in the subduction process. The spatial proximity of boninite ophiolites, in turn, indicates the possibility of mantle-crust interaction in the region and the activity of mantle-plume tectonics (Fig. 7).

The presence of ancient (533±4.6 Ma) inclusions of ultramafic (Ol-En) and eclogite (Jd-Grs) UHP rocks in the lower unit of the MC, structurally and genetically related to each other with formation parameters at T>700°C and P>3.5-4.4 GPa (Valizer et al. 2011, 2013a), suggests the involvement of mantle-crust sources and components involving diamond in the formation of the complex. However, geochemical data on the composition of rare and trace elements in the rocks of the complex indicate that the interaction of the mantle plume with the depleted mantle occurs in the pressure range of 3.5 to 2.0 GPa (Fig. 7). At this pressure, diamond, entering the region of formation of N-MORB and E_MORB compositions, becomes unstable, and the likelihood of its possible presence in the subduction process is significantly reduced.

The problem of diamond origin in the Maksyutov complex

Undoubtedly, the diamond is the main source of the problem of the origin and development of the Maksyutov complex, the main indicator of the conditions of ultra-high pressure during its formation. However, diamond discoveries in Maksyutov ccomplex rocks are quite rare and not always instrumentally confirmed. Only 2-3 nanosized grains in two eclogite samples as inclusions in garnet were studied by Raman spectroscopy (Bostick et al. 2003). Our repeated attempts to expand this search at the same university, using similar equipment, were unsuccessful. Reports of

isolated diamond finds in concentrates cannot be reliably proven to originate from prograde metamorphism. Cuboid graphite formations (Leech and Ernst 1998) typically form at low temperatures and are not associated with diamond graphitization (Korsakov et al. 2019).

Nevertheless, the maximum formation parameters of the rocks containing them, obtained by different methods and different authors, in different areas of the complex sometimes reach T = 800-910 ºC and P ~ 3.5-4.4 GPa (Valizer et al. 2013a; Fedkin et al. 2021). They certainly seem overestimated, especially since, with the indicated parameters, we can rightfully expect the appearance of trondhjemites and tonalities in the rocks of the complex - signs of slab melting, which are absent in the MC. The parameters of the upper critical point at P = 3.4 GPa and T = 760 ºC in the basalt-H_2O system explain their absence in the MC (Mibe et al. 2011). Most likely, the anomalous values of the P-T determinations indicate the participation in the formation of mantle-crustal inclusions of the complex, tectonically captured by the rising mantle plume at the peak of the subduction process. Traditional methods of metamorphic petrology were used to solve this problem within the framework of the development of the tectonic-petrological model of the complex.

Features of the evolution of the Maksyutov complex metamorphism

The metamorphism of the Maksyutov complex has been studied by many researchers (Lennykh, et al. 1995; Dobretsov et al. 1996; Leech, Ernst, 2000; Brown et al. 2006; Beane, Leech, 2007; Valizer et al. 2011, 2013a; Fedkin et al. 2021). A very wide range of formation parameters for the high-pressure rocks of the complex has been determined: from low-temperature greenschist associations to the top parameters of Ti-eclogites and mafic-ultramafic inclusions at T > 700-900 ºC and P up to 3.2-4.4 GPa. Our research and the work of Ural geologists (Valizer et al. 2011, 2013a; Kovalev et al. 2015; Rusin et al. 2021) confirmed the maximum metamorphic parameters of the complex: prograde stage - 800→900 °C, retrograde - 910→730 °C at P = 3.2-3.4 GPa.

It turned out that the main feature of MC metamorphism is not its extremely high parameters, but its cyclical, recurrent-pulsating nature (Fedkin, 2020), when prograde and retrograde metamorphism are repeated repeatedly, and the P-T trends constructed from the compositions of the Grt-Cpx-Pl-Qtz paragenesis form conjugate pairs characterizing the regimes of individual stages (cycles) of terrane development with prograde and retrograde branches of the trend. At least four such cycles have been recorded based on microprobe studies of the composition of coexisting MC phases (Table 1, Fig. 8).

Within each cycle (stage), the P-T parameters of the conjugate prograde and retrograde trends are virtually identical, and the time interval of inversion between them is virtually absent. The compositions and zoning of equilibrium mineral phases within a single paragenesis record the slightest changes in local equilibrium conditions (Fedkin, 2020). Garnet, due to its sensitivity to changes in crystallization conditions, records the parameters of several successive stages of metamorphic development, demonstrating them in individual samples, and sometimes even in a single large zoned grain with inverted zoning and a change in the direction of the P-T trend of its formation (Fedkin, 2024). Mutual prograde-retrograde transitions in a single sample or in a series of samples from a single outcrop are quite common in the MC. The P-T parameters of individual stages are repeated in virtually every section of the complex, sometimes simultaneously recording the metamorphic conditions of several cycles.

The time gap between metamorphic stages typically does not exceed 20-25 million years. Between the first and second cycles, it is ~150 million years. This gap marks a crucial turning point in the history of the Maksyutov complex – the transition from a subduction regime to terrane exhumation conditions, which follow one another within the common reconstructed subduction channel of the Maksyutov complex (Fig. 8).

The geochemical spectrum of eclogites for trace and trace elements in all areas shows a constant ratio of depleted and enriched compositions (in a ratio of ~1:2), regardless of the metamorphic grade, indicating a single process of formation of the entire complex in time and

518 space. Almost all rocks of the first cycle are enriched in high-field strength (HFSE) elements and
519 contain elevated niobium contents, while eclogites of lower metamorphic grades have nearly equal
520 ratios of these components. The statistical ratio of prograde and retrograde changes in the studied
521 samples (4:1) shows that the main direction of the complex's evolution was the subduction process
522 of subsidence with a small proportion of short-term reversible-regressive transformations during the
523 overall development of the complex. Traces of these PT oscillations are recorded in the composition
524 of zoned garnet in the Grt+Cp+Pl+Qz paragenesis as prograde tracks of individual samples.

525 Taken together, the prograde P-T trends of the initial stages of development form a general
526 trend of subduction-induced prograde subsidence of the complex, which ends with the final cycle 1
527 of high-pressure rock formation (Table 1; Fig. 8). Their ancient age (519-533 Ma) and maximum
528 formation parameters: T up to 790-910°C and P up to 3.3-3.5 GPa (Fedkin 2020), coincide with the
529 conditions of origin of the ultramafic-eclogite inclusions of the lower series in the area of the
530 village. Karayanovo: 533±4.6 Ma, T>700°C and P>3.5-4.4 GPa (Valizer et al. 2013a, 2015). These
531 parameters differ significantly from those of the preceding stages 2-4 (Table 1) and do not follow
532 the general pattern of geochemical development. The anomalous temporal, thermodynamic and
533 geochemical parameters of the cycle suggest that this stage is the result of mantle-crust interaction,
534 of a mantle wedge (plume?) that captured deep ultramafic-eclogite inclusions of a slab at the peak
535 of subduction and was brought to the surface as a result of tectonic ejecta during the transition
536 period from subduction to exhumation.

537 In terms of time and P-T parameters, this cycle marks the active period of the complex's
538 evolution—the moment of completion of subsidence and the beginning of terrane exhumation,
539 defining the overall duration of the entire retrograde stage—from the Early Paleozoic to the
540 Devonian inclusive. The complex's ascent likely occurred along a single, reconstructed subduction
541 channel, resulting in the thermodynamic parameters of subsidence and slab ascent being congruent,
542 and their signatures in the compositions of coexisting phases being virtually indistinguishable. This
543 is facilitated by the rapidity of the reciprocal pulsation mechanism. The period of inversion of the

local P-T trend within a single developmental stage is estimated at several million years (Leech and Stockli 2000). The statistical ratio of prograde and retrograde P-T changes in the high-pressure rocks of the complex (4:1) and their close mutual transitions indicate that traces of recurrent regressive changes were largely obscured by subsequent, more active subsidence processes, against which the trends and metrics of the MC cooling stage and its exhumation also became indistinguishable.

The causes of the occurrence and development of cyclical recurrent-pulsation metamorphism remain unclear. Various possible causes for this phenomenon include the rate of exhumation, the low thickness of the rising slab, its fluid saturation, or the high buoyancy of the rocks (Beane and Sorensen 2007). It is also unclear how the mechanism for the periodic uplift and subsidence of the UHP rock package is generated and operates at each stage of its development. It is likely that periodic dehydration of lawsonite due to temperature differences in deep subduction zones likely results in the replacement of lawsonite by less water-saturated (lighter) aggregates of clinozoisite, albite, garnet, chlorite, white micas, and titanite (Clarke et al. 2006; Chen et al. 2013). Consequently, the lawsonite dehydration reaction reduces the density of the slab and increases its buoyancy.

The specific nature of recurrent pulsation metamorphism in the MC region—heterogeneity at high pressure—has demonstrated the potential of thermobarometry for studying local petrologic complexes and identifying anomalous zones and inclusions containing diamond and coesite. Such zones of petrologic heterogeneity are associated with increased mantle-crust interaction and the appearance of high-pressure phases such as diamond and coesite within shallow metaterrigenous complexes, as well as elevated first-level mineral formation parameters (Table 1).

Deep-seated inclusions of ultramafic rocks and tectonic-petrological model of the Maksyutov complex

The issues and problems discussed in the analysis of the geochemical, petrologic, and geodynamic features of the Maksyutov terrane during the development of the tectonic-petrological model pertain exclusively to its internal features and do not address the essence of the subduction initiation problem. At the same time, to achieve full compliance of the Maksyutov terrane with the SIR criteria, it is necessary to confirm the key features of the chemostratigraphic sequence of the formation of the ophiolite portion of the complex: the original basaltic composition of the metabasites that make up the bulk of the unit and the absence of metamorphic and metasomatic alteration (Whattam and Stern 2011). Unfortunately, it is not possible to obtain this data promptly, as the original basalts have not been preserved in the upper ophiolite block of the Maksyutov terrane. Under the influence of metasomatic processes, they were replaced by greenstones and schists, and in the interlayers and blocks of the host metasedimentary rocks, bodies of already altered metasomatites, serpentinite mélange, mafic and ultramafic inclusions, lawsonite rocks, and eclogites are described (Valizer et al. 2013b; Rusin et al. 2021). Partial information on the chemostratigraphic sequence of the ophiolite complex can be found in the general geochemical material on the metabasite formations of the lower unit of the complex. But this information cannot replace a strict chemostratigraphic sequence of SIR, and we cannot accept full compliance with the SIR rules in the rocks of the Maksyutov complex, but only partial compliance.

It is assumed that during the long history of its formation, the MC has gone through different stages of its development: the state of the oceanic crust, rifting, collisional and subduction processes, the transformation of the oceanic crust into continental crust, suprasubduction changes, etc. (Dobretsov et al. 1996; Lennykhet al. 1995; Puchkov 1993; and others). Most researchers believe that the Maksyutov complex formed during the late Paleozoic convergence, when the East European Platform collided with microcontinental fragments of the Magnitogorsk island arc located along the western margin of the Siberian Craton (Zonenshain et al. 1984; Dobretsov et al. 1996; Puchkov 1997). Thus, the upper unit of the complex is interpreted as a metaophiolitic mélange, while the structurally lower lithologic series may represent segments of an older microcontinent in

596 the deep zone of a continental rift (Valizer et al. 2013b; Dobretsov 1991; Dobretsov et al. 1996;
597 Rusin 2007). The age of its formation is ~ 470-440 Ma. The complex, exhumed as a result of
598 tectonic mélange, probably rose from the depths of the subduction zone due to its buoyancy relative
599 to the surrounding mantle (Matte and Chemenda 1996; Ernst et al. 1997) during the unification of
600 all structural elements of the terrane into a single Maksyutovsky complex - 372-390 Ma (Glodny et
601 al. 2002; Rusin 2007; Rusin et al. 2021).

602 The assumed change in the polarity of the MC subduction and the pulsating nature of
603 metamorphism could, during the process of subsidence and exhumation of the complex, lead to
604 mixing and equalization of the compositions of metabasic rocks of the continental and ophiolite
605 parts of the complex, recording the most stable features of the chemostratigraphic sequence of their
606 changes. As a result, its constituent structural and material units, inclusions, and blocks, formed in
607 different tectonic settings, were combined and mixed within a single subduction channel at the
608 onset of orogeny in the Early Devonian (Brown et al. 2006; Puchkov 2010).

609 Ultramafic (Ol-En and En) inclusions of this age in quartzite schists of the lower unit were
610 formed in the deep zone of the continental rift and advanced into the crustal subduction zone as a
611 result of tectonic mélange, the age of which is close to the age of the unification of all structural
612 elements of the terrane into a single Maksyutov complex - 372-390 Ma (Glodny et al. 2002; Rusin
613 2007; Rusin et al. 2021).

614 It is surprising that, in such a short time, the rocks of the complex evolved from tholeiitic
615 basalts to calc-alkaline ones (Fig. 3), changing their mantle source from N-MORB to OIB type (Fig.
616 4), changing the ratio of enriched and depleted compositions to a ratio of 2:1, and demonstrating the
617 absence of any anomalies in the spectra of rare earth elements (Fig. 5). These and other
618 geochemical features of the eclogites of the complex should certainly be considered important
619 indicators of the chemostratigraphic sequence of the evolution of the composition of the original
620 rocks. Some of these, such as the ratio of trace and minor elements in the rocks of the MC, allowed
621 us to estimate for the first time for this terrane the contribution of the subduction component (from

1.0 to 4%) as the subduction initiation process developed (Fig. 6), to establish the nature of the interaction of the mantle plume with the depleted mantle, as well as the degree of partial melting in the formation zone of the N-MORB and E-MORB compositions (Fig. 7), etc. Thus, the main features of the chemostratigraphic sequence of the compositional evolution of the original rocks of the complex are taken into account in this work, and this important criterion of the SIR can be considered fulfilled to a certain extent.

It is noteworthy that significant metasomatic changes in the compositions of the rocks of the lower unit of the complex do not occur. At the initial (prograde) stage of its development, the composition of high-pressure rocks of the eclogite-schist part remains virtually unchanged (Beane and Sorensen 2007; Dobretsov et al. 1996; Lennykh et al. 1995; Volkova et al. 2004). Metasomatism of mafic-ultramafic rocks is hindered by the pulsating nature of metamorphism and the high buoyancy of the subducting plate (Leech and Ernst 2000; Schulte and Blümel 1999). The first signs of metasomatism in the lower basite member appear only at the regressive stages of metamorphism in the form of muscovite zones, veinlet accumulations of zoned garnets, and chlorite rims around it. Garnet acquires complex, multidirectional, and sometimes inversion zoning. The grains exhibit textures of atoll and openwork garnet, confirming the presence of fluid (Beane and Sorensen 2007). Low-temperature phases of Zo, Gln, and Chl in eclogite associations appear as a result of metasomatic processes only in the third stage at temperatures below 460–430°C (Valizer et al. 2011).

The upper ophiolite unit of the Maksyutov complex has its own history of development, starting from the time of the origin of its supposed substrate at 1660±10 Ma or, according to more precise data, at 824 Ma (Valizer et al. 2011, 2013b) to the time of its unification with the rocks of the eclogite-glaucophane schist part: 390 Ma is the time accepted by the opinion of the majority of researchers; 372-341 Ma according to the data of (Valizer et al. 2013b); 380-385 Ma are our data (Table 1, 3rd stage), which record the maximum age of prograde HP metamorphism. The upper unit of the MC is dominated by greenstones and schists, ancient mélange rocks at the base, with

antigorite serpentinites, Ca-eclogites, lawsonite-bearing rocks, and metabasites (Valizer and Lennykh 1988).

Among the metasomatites and mafic rocks, individual inclusions and blocks of earlier origin are distinguished, predating the amalgamation of the upper and lower units into a single complex. These inclusions include Grt-Cpx and Law-bearing rocks with a very rare Fe-Ca garnet paragenesis (Valizer et al. 2013b). Their formation age is 470 Ma, and their diaphthoresis age is 440 Ma. Rocks of this series are also considered high-pressure formations of the deep continental rift zone and are distinguished as a separate "mafic-ultramafic" unit. The range of PT parameters for the formation of these rocks is quite wide: from 620-760 °C and 2.5-4.0 GPa for the Law+Zo paragenesis (Schmidt and Poli 1994) to T=380-467 °C and P=0.7-1.1 GPa for the retrograde replacement of lawsonite by clinozoisite, muscovite, calcite, and albite. This suggests that various ancient mantle-crustal formations with parameters in the UHP stability range of the minerals diamond and coesite participated in the formation of the Maksyutov complex long before its subduction. Exactly the same age range (471–444 Ma) was established for the crystallization of Law eclogite in the Utarbaevskaya association of diopside-grossular metasomatites and lawsonite eclogites, in which coesite microinclusions were found in omphacite grains (Rusin et al. 2021). The stability of coesite is confirmed by the Raman spectra of the mineral and indicates fairly high formation parameters of the Law paragenesis: T = 495–622 °C at P = 2.2–2.4 GPa (Grt-Omp, Grt-Omp-Ph thermobarometry), which also gives reason to believe that these rocks may have participated in the pre-subduction development of the MC. The older age of the coesite-bearing rocks of the Utarbaevo association and the "mafic-ultramafic" unit compared to the completion of the MC subduction (~341-390 Ma) places these units in the category of similar mantle-crustal inclusions of the lower structural-material unit of the MC (Valizer et al. 2011, 2013a).

The most contrasting position between the eclogite and ophiolitic parts of the MC is occupied by exotic metaultramafics (antigorite metaharzburgites and metaorthopyroxenite), which formed as a result of high-pressure Si-Al metasomatism at 630°C and 2.0 GPa (Perchuk et al.

2024). Since metasomatism has not been established in the host eclogites, garnet-mica schists, and quartzites (Dobretsov et al. 1996; Lennykh et al. 1995; Valizer et al. 2011, 2013a, 2013b), it is believed that Si-Al metasomatism occurred in the subduction channel before their tectonic juxtaposition with the rest of the crustal rocks (Perchuk et al. 2024). The authors believe that these meta-ultramafics are fragments of the suprasubduction mantle, tectonically juxtaposed with eclogites and metasedimentary rocks of the subducting plate. Previously, the hypothesis of suprasubduction-related changes in the MC oceanic lithosphere was considered in connection with the formation of the Early Devonian P-MORB ridge in the Southern Urals during the Ordovician (Ryazantsev et al. 2008). Thus, the age interval of 470–440 Ma represents an important boundary in the development of the MC ophiolite unit.

The history of antigorite meta-ultramafics resembles the aforementioned Ol-En inclusions in the lower part of the Maksyutov complex, which are genetically related to Jd-Gros eclogites (Valizer et al. 2013a, 2015), though they differ in their formation age and geodynamic setting. Ol-En inclusions formed (or were trapped by a mantle plume) in the deep zone of a continental rift, while antigorite meta-ultramafics represent oceanic crust that underwent suprasubduction alteration (Si-Al metasomatism, serpentinite mélange) prior to the onset of subduction and the final formation of the ophiolite complex in the Early Devonian.

Deep inclusions of mafic and ultramafic rocks, high-pressure metasomatites, lawsonite rocks, and eclogites shaped the Maksyutov complex long before its subduction. These included inclusions containing diamond and coesite, as well as mafic and ultramafic mineral assemblages extruded to the surface within a mantle plume/wedge. The PT conditions of prograde subduction did not reach the diamond and coesite stability region, therefore their origin cannot be considered ultra-high-pressure (UHP).

CONCLUSION

Studies conducted to test the "Subduction Initiation Rule" concept (Whattam and Stern 2011; Whattam 2023) at the Maksyutov complex have shown that the main features of subduction are the temporal and spatial combination of eclogite and ophiolite formation; key features of the chemostratigraphic sequence; and the presence of a reconstructed HP/UHP subduction channel. These features are clearly reflected in the structure and rocks of the Maksyutov complex, confirming the proposed model of subduction initiation as a universal concept for crustal eclogite formation. In the course of the conducted research, based on new data on the chemical composition of the high-pressure rocks of the complex (Fedkin et al., 2021), the proposed concept of "Subduction Initiation Rules" (Whattam and Stern 2011; Whattam 2023), and the geodynamic classification of oceanic basalts (Pearce 2008), some additional conditions and parameters for the initiation and development of the subduction process were determined for the first time for the Maksyutov complex, expanding its main characteristics.

1. The formation of HP-UHP rocks of the MC requires at least a three-component source material: enriched OIB mantle, depleted mantle, and some contribution from the subduction component (crustal contamination).

2. It was established that the composition of the primary melt of the complex has a variable from tholeiitic to calc-alkaline series and further to andesite-basalt. The composition of rocks in this series becomes increasingly depleted in coherent elements due to fluid influx and increasing oxidation levels (Whattam 2023).

3. New geochemical data on the HP-UHP composition of MC rocks for rare and trace elements allowed us to estimate the contribution of the subduction component in MC rocks from 1 to 4%. This sheds new light on the history of the origin and development of the Ural Ocean Basin and the significance of suprasubduction changes in the oceanic lithosphere in the Southern Urals during the Ordovician.

4. For the first time, a pressure range of 1.5-3.5 GPa for mantle-crust interaction and magma generation in a mantle plume (at $P < 3.5$ GPa in OIB basalts) and in the depleted mantle at $P \leq 1.5$ GPa during the formation of E-MORB and N_MORB melts was determined for MC.

5. The cyclical, recurrent-pulsational nature of the Maksyutov complex's metamorphism determines the presence of high-pressure minerals—diamond and coesite—in its rocks as a result of their capture by a mantle plume at P-T parameters exceeding their stability limits. Their origin through in situ progressive metamorphism during terrane subduction has not been confirmed, and the ultra-high-pressure (UHP) status of the Maksyutov complex cannot be considered sufficiently substantiated.

Acknowledgments The work was supported by the Laboratory of Metamorphism, Magmatism and Geodynamics of the Lithosphere at the D.S. Korzhinsky Institute of Experimental Mineralogy, Russian Academy of Sciences within the framework of the State Assignment FMUF-2022-0004, No. 1021051302305-5-1.5.2; 1.5.4, and the Fulbright Grant of the Institute of International Education, 2012-2015. The authors express their deep and sincere gratitude to Stanford University staff members, Prof. Gary Ernst (Prof. W.G. Ernst) and University of San Francisco Prof. Mary Leech (Prof. M. Leech) for initiating this research, support and assistance in the work.

References

Beane R, Sorensen SS (2007) Protolith signatures and element mobility of the Maksyutov subducted slab, Southern Ural Mountains, Russia: Inter. Geol. Review, 49:52-72

Beane RJ, Leech ML (2007) The Maksyutov complex: The first UHP terrane 40 years later. In Cloos M, Carlson WD, Gilbert MC, Liou JG. Sorensen SS (eds.) Convergent Margin

750 Terranes and Associated Regions: A Tribute to W.G. Ernst Geological Society of America
751 Special Paper (419):153-169. doi: 10.1130/2006.2419(08)
752 Bostick BC, Jones RE, Ernst WG et al. (2003) Positive identification of microdiamond from the
753 Maksyutov Complex, south Urals, Russia. American Mineralogist 88:1709-1717
754 Brown D, Juhlin C, Alvarez-Marron J, Pérez-Estaún A, and Oslianski A, 1998, Crustal-scale
755 structure and evolution of an arc-continent collision zone in the southern Urals, Russia:
756 Tectonics, v. 17, p. 158–171
757 Brown D, Spadea P, Puchkov V, Alvarez-Marron J, Herrington R, Willner AP, Hetzer R,
758 Gorozhanina Yu, Juhlin C (2006) Arc-continent collision in the Southern Urals. Earth-
759 Science Reviews 79:261–287
760 Chen Y, Ye K, Wu TF, Guo S (2013) Exhumation of oceanic eclogites: thermodynamic constraints
761 on pressure, temperature, bulk composition and density. *J. Metamorph. Geol* **31**:549-570
762 Chesnokov BV, Popov VA (1965) Increasing Volume of Quartz Grains in the Eclogites of Southern
763 Urals. Dokl. Akad. Nauk SSSR 162(4):909–910
764 Clarke GL, Powell R, Fitzherbert IA (2006) The lawsonite paradox: a comparison of field evidence
765 and mineral equilibria modeling. *J. Metamorph. Geol* 24:715-725. DOI: 10.1111/j.1525-
766 1314.2006.00664.x
767 Colpron M, McClelland WC, Piercey SJ, et al. (2025) Revisiting the “Klondike Orogeny”: Permian
768 to Jurassic Development of the Yukon-Tanana Terrane, Northern Canadian Cordillera.
769 Tectonics 44(6). https://doi.org/10.1029/2024TC008748
770 Creaser RA, Goodwin-Bell JAS, Erdmer P (1999) Geochemical and Nd isotope constraints for
771 the origin of eclogite protoliths, Northern Cordillera: Implications for the Paleozoic
772 tectonic evolution of the Yukon-Tanana terrane. Canadian Journal of Earth Sciences
773 36:1697–1709, https://doi.org/10.1139/e99-070
774 Dobretsov NL (1974) Glaucophane_schist and Eclogite Glaucopahne_schist Complexes of the
775 USSR. Nauka, Novosibirsk (in Russian)

776 Dobretsov NL, Shatsky VS, Coleman RG et al. (1996) Tectonic setting of ultrahigh-pressure
777 metamorphic rocks in the Maksutov Complex, Ural Mountains, Russia. Intern. Geology
778 Review 38:136-160
779 Ernst WG, MaruyamaS, and Wallis S (1997) Buoyancy-driven, rapid exhumation of ultrahigh-
780 pressure metamorphosed continental crust: Proceedings of the National Academy of
781 Sciences 94: 9532-9537
782 Fedkin VV, Leech, ML, Shchipansky AA, Burlick TD, Valizer PM, Ernst WG (2017), Coexisting
783 zoned garnets and clinopyroxenes from mafic eclogites of the Maksyutov Complex, South
784 Ural Mountains, Russia. Experiment in Geosciences 23(1): 1-10
785 Fedkin VV (2020) Four Stages of the Thermal Evolution of Eclogites from the Maksyutov
786 Complex (South Urals). Russian Geology and Geophysics 61(5-6):543–558.
787 doi:10.15372/RGG2019182
788 Fedkin VV (2024) Zonal garnets of eclogite-blueschist complexes - recorder of the history of their
789 development. J.Mari.Scie.Res.Ocean. 7(1):01-12 DOI: 10.33140/JMSRO.07.01
790 Fedkin VV, Burlick TD, Leech ML, Shchipansky AA, Valizer PM, Ernst WG (2021) Petrotectonic
791 origin of mafic eclogites from the Maksyutov subduction complex, south Ural Mountains,
792 Russia. In Wakabayashi J, Dilek Y (eds.) Plate Tectonics, Ophiolites, and Societal
793 Significance of Geology. Geological Society of America Special Paper 552: 177–195.
794 https://doi.org/10.1130/2021.2552(09)
795 Korsakov AV, et al. (2019) Natural graphite cuboids. Minerals 9(2):110-115.
796 DOI: 10.3390/min9020110
797 Kovalev SG, Timofeeva EA, Pindyurina EO (2015) Geochemistry of Eclogites of the Maksutov
798 complex (Southern Urals) and Genetic Nature of their Protoliths. Geochemistry (4):299-327.
799 DOI: 10.7868/S0016752515040044 (in Russian)
800 Kuzmin MI, Kabanova LYa (1991) Boninite series of the Southern Urals: geological and
801 petrographic description, compositional features, and problems of origin. In: Potential ore

content, geochemical types, and formations of igneous rocks. Nauka, Novosibirsk, 156–173 (in Russian)

Glodny J, BingenB, Austrheim H, Molina JF, Rusin A (2002) Precise eclogitization ages deduced from Rb/Sr mineral systematics: The Maksyutov Complex, Southern Urals, Russia: Geochimica et Cosmochimica Acta 66: 1221-1232

Le Bas MJ, Streckeisen AL (1991) The IUGS systematics of igneous rocks. Jour. Geol. Soc. London 148:825-833

Leech ML, Ernst WG (1998) Graphite Pseudomorphs After Diamond? A Carbon Isotope and Spectroscopic Study of Graphite Cuboids from the Maksyutov Complex, South Ural Mountains, Russia. Geochim. Cosmochim. Acta 62: 2143–2154

Leech ML, Ernst WG (2000) Petrotectonic evolution of the high- to ultrahigh- pressure Maksyutov Complex, Karayanova area, south Ural Mountains, Russia: structural and oxygen isotopic constraints. Lithos 52:235-252

Leech ML, Stockli DF (2000) The late exhumation history of the ultrahigh-pressure Maksyutov Complex, south Ural Mountains, from new apatite fission track data. Tectonics 19:153–167. doi: 10.1029/1999TC900053

Leech ML Willingshofer E (2004) Thermal modeling of an ultrahigh-pressure complex in the south Urals: Earth and Planetary Science Letters 226: 85-99

Lennykh VI, Valizer PM (1999), High-pressure metamorphic rocks of the Maksyutov complex (Southern Urals). In: Proceedings, 4th international eclogite field symposium. Russian Academy of Sciences, Novosibirsk, 64 p

Lennykh VI, Valizer PM, Beane R, Leech M, Ernst WG (1995) Petrotectonic evolution of the Maksyutov complex, southern Urals, Russia: Implications for ultrahigh-pressure metamorphism. International Geology Review 37: 584–600. https://doi.org/10.1080/00206819509465420

827 Liou JG, Zhang RY, Ernst WG, Rumble DIII, Maruyama S (1998) High pressure minerals from
828 deeply subducted metamorphic rocks. Rev. Mineral 37:33-96
829 Matte VV (1984) Plate tectonic model of the South Urals development: TectonophysicsP., and
830 Chemenda, A., 1996, A mechanism for exhumation of high pressure metamorphic rocks
831 during continental subduction in southern Urals: Comptes Rendu Academie des Sciences de
832 Paris 323: II 525-530.
833 Meschede M (1986) A method of discriminating between different types of mid0oceanridge basalts
834 and continental tholeiites with the Nb-Zr-Y diagram. Chemical Geology 56: 207-218
835 Mibe K, Kawamoto T, Matsukage KN, Fei Y, Ono S (2011) Slab melting versus slab dehydration
836 in subduction-zone Magmatism. Proceedings of the National of Sciences108: 8177-8182
837 Mullen D (1983) MnO/NiO2/P2O5: a minor element discriminant for basaltic rocks of oceanic
838 environments and its implications for petrogenesis. Earth and Planetary Science Letters
839 62:53-62
840 Pearce JA (2008) Geochemical fingerprinting of oceanic basalts with applications to ophiolite
841 classification and the search for Archean oceanic crust. Lithos 100:14-48
842 Perchuk AL (1992) A new version of the omphacite-albite-quartz geobarometer taking into account
843 the structural states of omphacite and albite. Dokl. RAS USSR 324:1286–1189 (in Russian)
844 37
845 Perchuk AL, Zinovieva NG, Sapegina AV, Valizer PM, Kozlovsky VM, Grigorieva VM,
846 Podgornova ST (2024) Metaultramafics of the Maksyutovsky complex, Southern Urals:
847 high-pressure Si-Al metasomatism and carbonatization at the crust-mantle boundary in the
848 subduction zone. Petrology 32: 59–90. (in Russian)
849 Perchuk LL, Lavrent'eva IV, Aranovich LYa, Podlesskii KK (1983) Biotite–Garnet–Cordierite
850 Equilibria and Evolution of Metamorphism Nauka, Moscow (in Russian)

Powell R (1985) Regression diagnostics and robust regression in geothermometer/geobarometer calibration: the garnet-clinopyroxene Geothermometer revisited. J. Metamorph. Geol. 3:231-243

Puchkov VN (2010) Geology of the Urals and Cis-Urals (actual problems of stratigraphy, tectonics, geodynamics and metallogeny). DesignPoligraphService Publ Ufa: 280 pp. (in Russian)

Rusin AI, Zvorygina AA, Valizer PM (2021) Lawsonite eclogites and metasomatites of the Utarbaevo association of the Maksyutov complex. Lithosphere. 21(6):867–883. https://doi.org/10.24930/1681-9004-2021-21-6-867-883. (in Russian)

Ryazantsev AV, Tolmacheva TYu (2016) Ordovician volcanic and plutonic complexes of the Sakmara allochthon in the Southern Urals. Geotectonics 50(6): 23-51. DOI: 10.1134/S0016852116060066

Ryazantsev AV, Dubinina SV, Kuznetsov NB, Belova AA (2008) Ordovician lithotectonic complexes in allochtons of the Southern Urals. Geotectonics 5:368-395

Schmidt MW, Poli S (1994) The stability of lawsonite and zoisite at high pressures: experiments in CASH to 92 kbar and implications for the presence of hydrous phases in subducted lithosphere. Earth Planet. Sci. Lett 124:105-118

Shatsky VS, Jagoutz E, Koz'menko OA (1997) Sm-Nd dating of the high-pressure metamorphism of the Maksyutov Complex, southern Urals. Transactions (Doklady) of the Russian Academy of Sciences, Earth Science Section 353: 285-288

Spadea P, D'Antonio M (2006) Initiation and evolution of intra-oceanic subduction in the Uralides: geochemical and isotopic constrains from Devonian oceanic rocks of the Southern Urals, Russia. Island Arcs 15: 7-25.

Sun SS, McDonough WF (1989) Chemical and isotopic systematics of oceanic basalts: implication for mantle composition and processes in Magmatism in the ocean basins. Geological Society, Special Publication 42: 313-345

876 Taylor SR, McLennan SM (1985) The continental crust: its composition and evolution. Blackwell,
877 Oxford, 312 p.
878 Valiser PM, Lennykh VI (1988) Amphiboles of Blue Schists of the Urals, (Nauka, Moscow) (in
879 Russian)
880 Valizer PM, Krasnobaev AA, Rusin AI (2011) Ultrahigh-Pressure (UHP) associations in
881 ultramafites of the Maksyutov complex (southern Urals). Doklady Earth Sci. 441: 1645-
882 1648
883 Valizer PM, Krasnobaev AA, Rusin AI (2015) UHPM Eclogite of the Maksyutov
884 Complex (Southern Urals). Doklady Earth Sci. 461(1): 291-296. doi:
885 10.1134/S1028334X1503023X
886 Valizer PM, Krasnobaev AA, Rusin AI (2013) Jadeite-grossular eclogite of the Maksyutov
887 Complex (Southern Ural). Lithosphera 4:50-61 (in Russian)
888 Volkova NL, Frenkel AE, Budanov VI, Lepezin GG (2004) Geochemical signatures for eclogite
889 protolith from the Maksyutov Complex, South Urals. Journal of Asian Earth Sciences. 23:
890 745-759. DOI https://doi.org/10.1016/S1367-120(03)00128-7
891 Whattam SA (2023) Subduction initiation ophiolites of the SW Pacific I: first-formed MORB-like
892 lavas. International Geology Review. DOI: 10.1080/00206814.2023.2248489
893 Whattam SA, Stern RJ (2011) The 'subduction initiation rule': a key for linking ophiolite, intra-
894 oceanic forearcs, and subduction initiation. Contrib. Mineral. Petrol. 1031–1045
895 Wood DA (1980) The application of a Th-Hf-Ta diagram to problem of tectonomagmatic
896 classification and to establishing the nature of crustal contamination of basaltic lavas of the
897 British Tertiary volcanic province. Earth and Planetary Science Letters 50:11
898 Zacharov OA, (1991) New data on the geological structure of the Maksyutov amorphosed complex
899 in the upper part of the Sakmara River. *in* Overthrust-Nappe Tectonics and its Role in the
900 Formation of Natural Deposits: IG BNTS UrO, USSR Academy of Sciences, Ufa.

Zonenshain LP, Korinevsky VG, Kazmin VG, Pecherskiy DM, Khain VV, and Matveyenkov VV, (1984) Plate tectonic model of the South Urals development: Tectonophysics 109: 95-135.

Figures

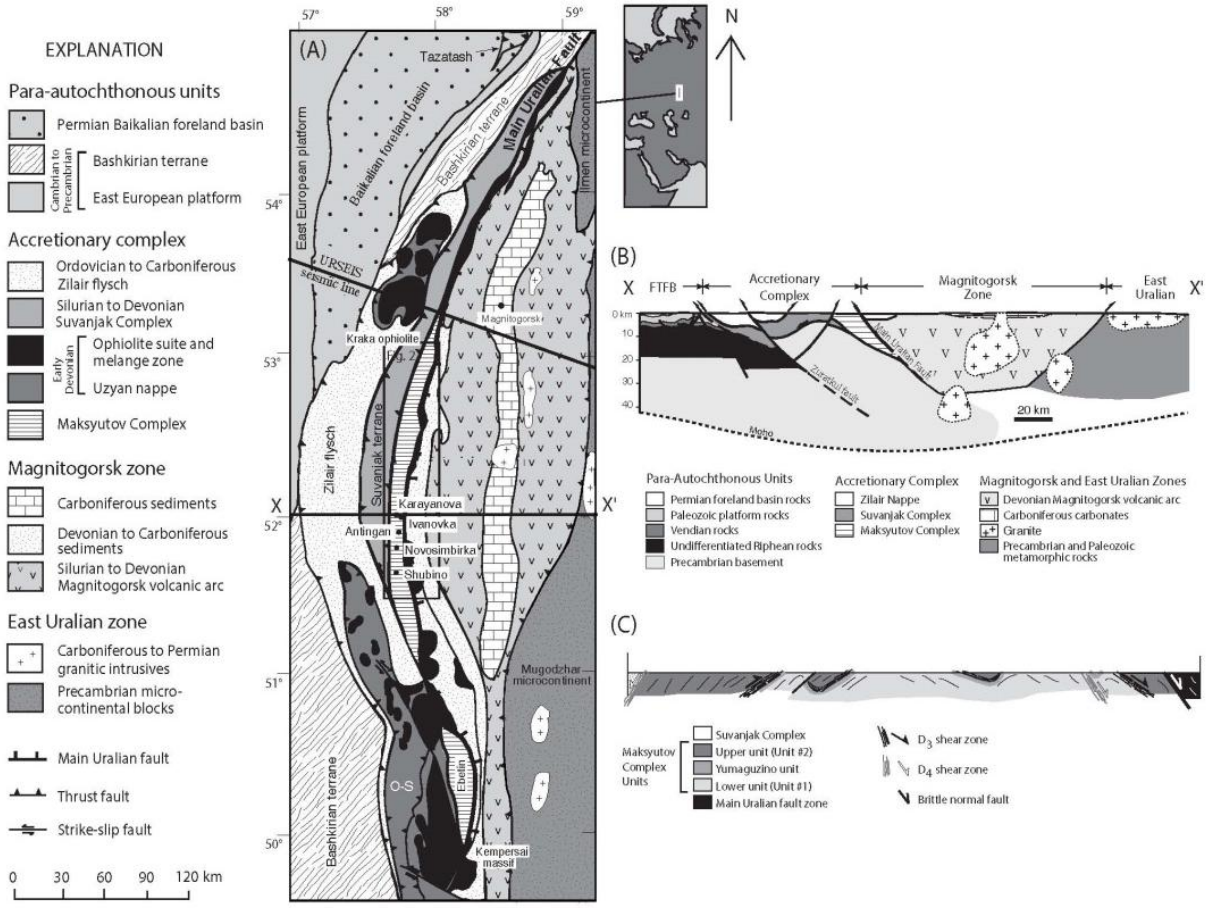
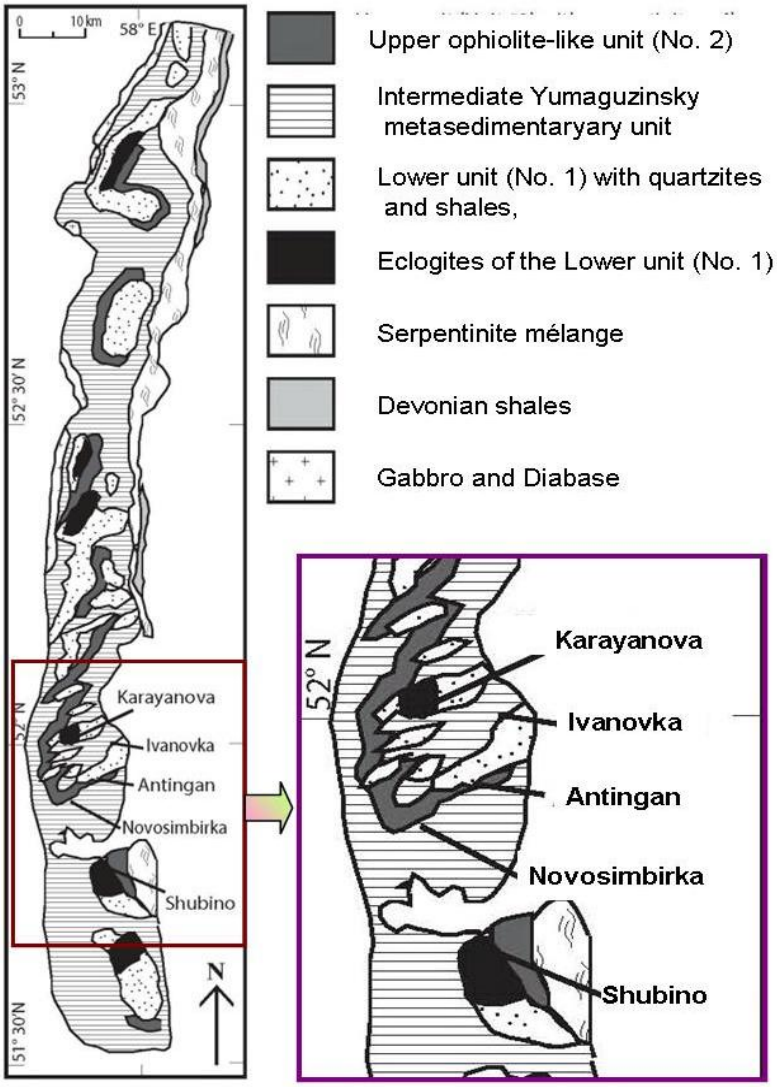


Fig. 1 Geotectonic map of the South Ural Mountains, Russia (Latitude & Longitude N51°30'00" - N53°00'00", E58°00'00" - E58°00'00"), adapted from (Leech and Stockli, 2000) with the URSEIS (Urals reflection seismic experiment and integrated studies) transect that provides important depth control for the South Ural Mountains and with additions by the authors

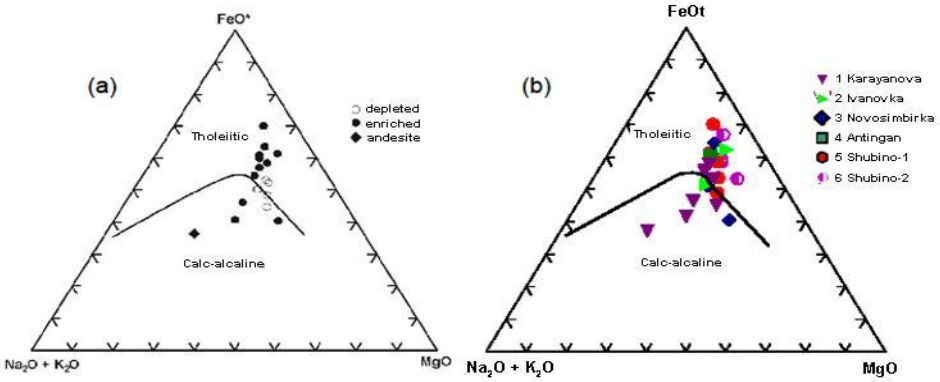


913

914 **Fig. 2** Lithological-tectonic units of the Maksyutov complex (Lennykh and Valizer 1999)

915 with sampling locations in the southern part of the terrane (Fedkin et al. 2021)

916



917

918 **Fig. 3** Compositional range of Maksyutov eclogites plotted in an AFM diagram

(a) Bulk-rock compositions; (b) Position of the analyzed samples from different locations

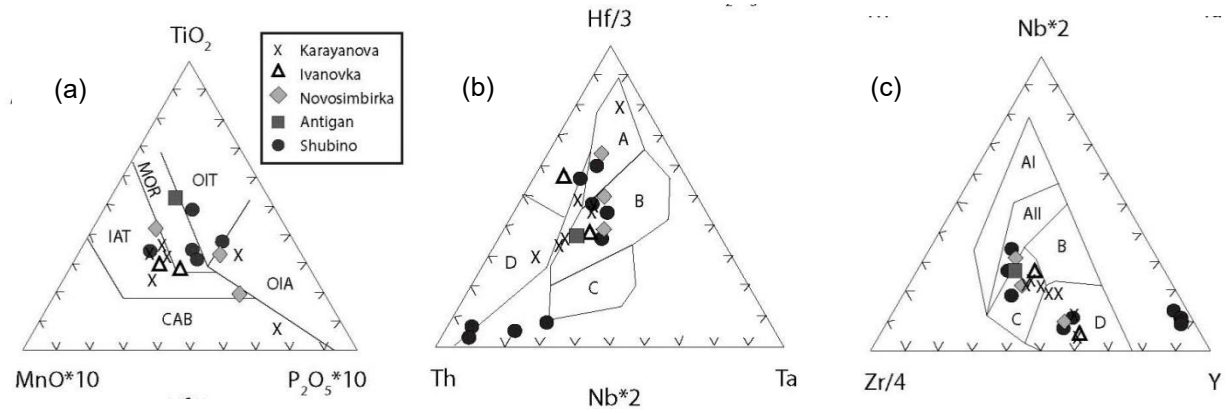


Fig. 4 Discrimination diagrams of the studied eclogite samples of the Maksyutov complex in different coordinates and sampling location

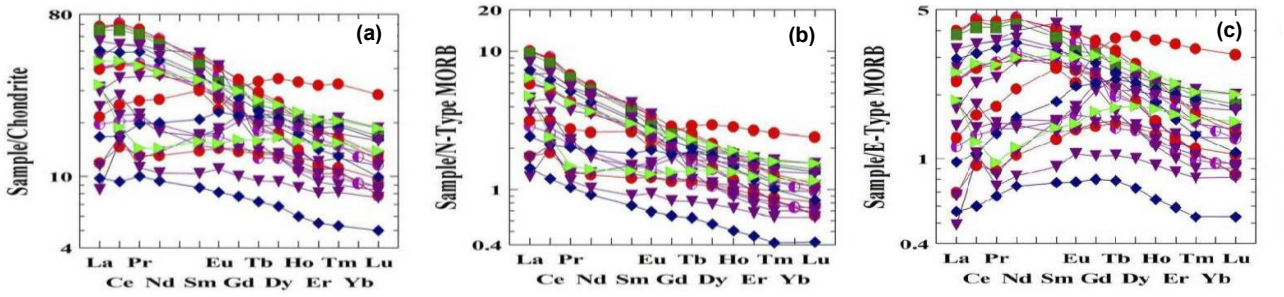


Fig. 5 The REE variation diagrams for analyzed Maksyutov eclogitic rocks (Fedkin et al. 2021) normalized to chondrite (a) after (Mullen 1983; Taylor and McLennan 1985), to N-type MORB (b) and E-type MORB (c) after (Sun, McDonough 1989). Sampling location designations are the same as in Fig. 3b

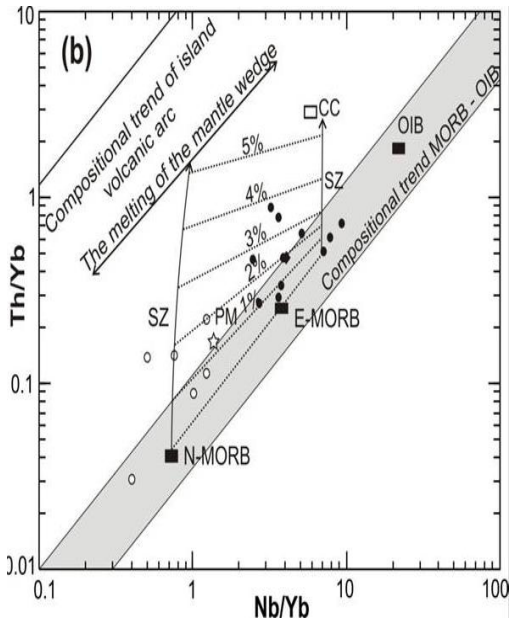
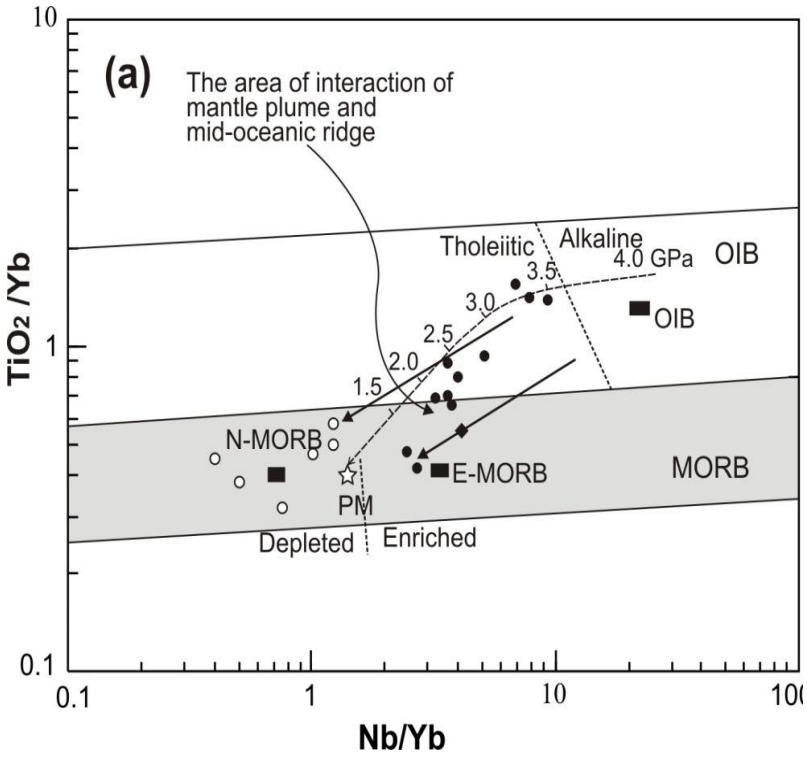


Fig. 6 Contribution of the subduction component in high-pressure rocks of the MC

Compositions of eclogites of the Maksyutov complex: enriched – filled circles and depleted – open circles. (Fedkin et al. 2021) on the Th/Yb–Nb/Yb diagram (Pearce, 2008). Parameters are indicated in ppm



941

942

943 **Fig. 7** Interaction of the OIB-type mantle plume with the MORB-type depleted mantle.

944 Compositions of eclogites of the Maksyutov complex after (Fedkin et al. 2021) on the

945 TiO_2/Yb–Nb/Yb diagram (Pearce, 2008). Parameters are indicated in ppm

946

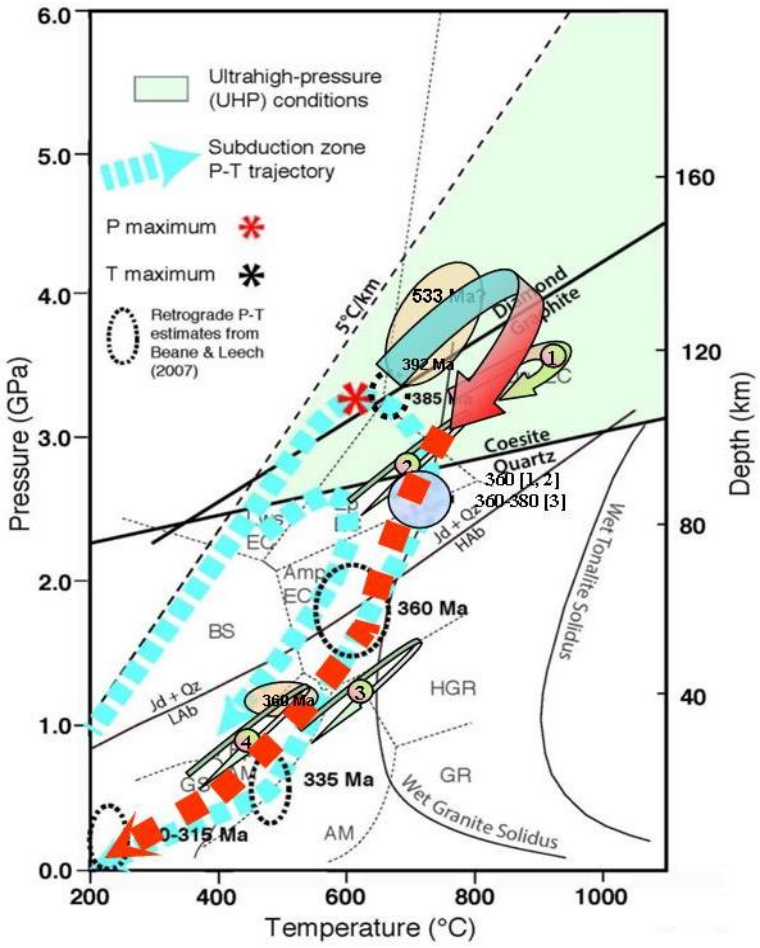


Fig. 8 Physicochemical conditions of the formation of the Maksyutov complex (Fedkin, 2020). Petrogenetic fields of metabasic rocks (Liou et al. 1998): EC - eclogites, DS - blueschists, GR - granulites, HGR - high- pressure granulites, AM, amphibolites. Numbers 1-4 in circles are prograde-retrograde cycles of metamorphism evolution

Table 1. Generalized RT trends of prograde-retrograde stages (cycles) of development of the Maksyutov eclogite-blueschist complex (Fedkin 2020)

Stage No	Prograde trends	Retrograde trends	Age, Ma*
1.	T=800→900 °C, P=3,5 GPa	T=910→730 °C, P=3,5 GPa	515-533 [1])
2.	T=500→790 °C, P=2,5→3,0 GPa	T=740→610 °C, P=2,5→1,4 GPa	360-385 [1]), [2]) 360-380 [3])
3.	T=460→680 °C, P=1,1→1,5 GPa	T=690→430 °C, P=1,3→1,0 GPa	335 [2])
4.	T=310→515 °C, P=0,9→1,2 GPa	T=545→310 °C, P=1,0→0,6 GPa	310-315 [2])

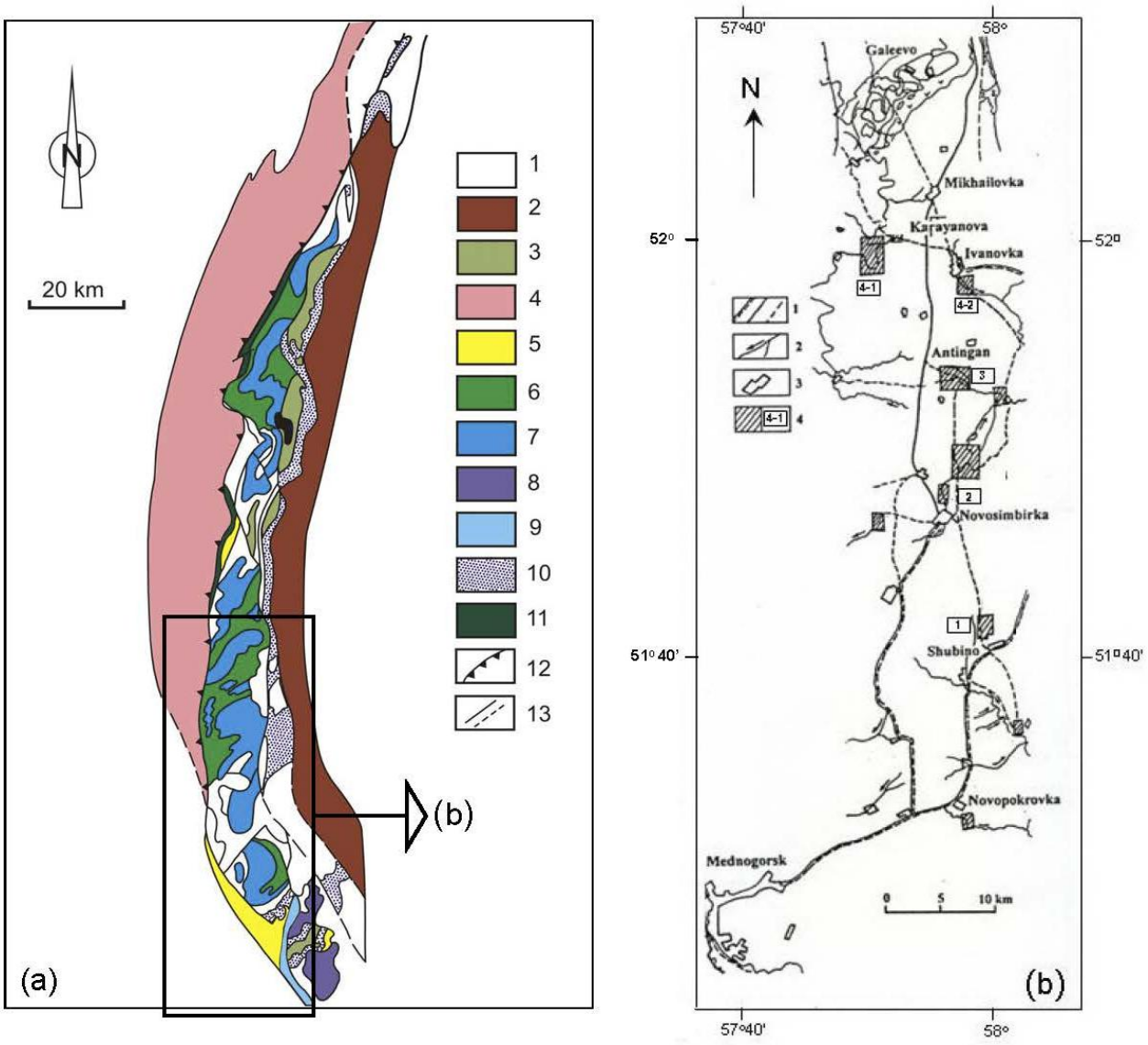
959 *) Age determinations are given after: [1]) Valizer et al. 2013a, [2]) Beane, Leech, 2007, [3])

960 Dobretsov et al. 1996.

961

962 **Supplementary Materials 1 (SM-1)**

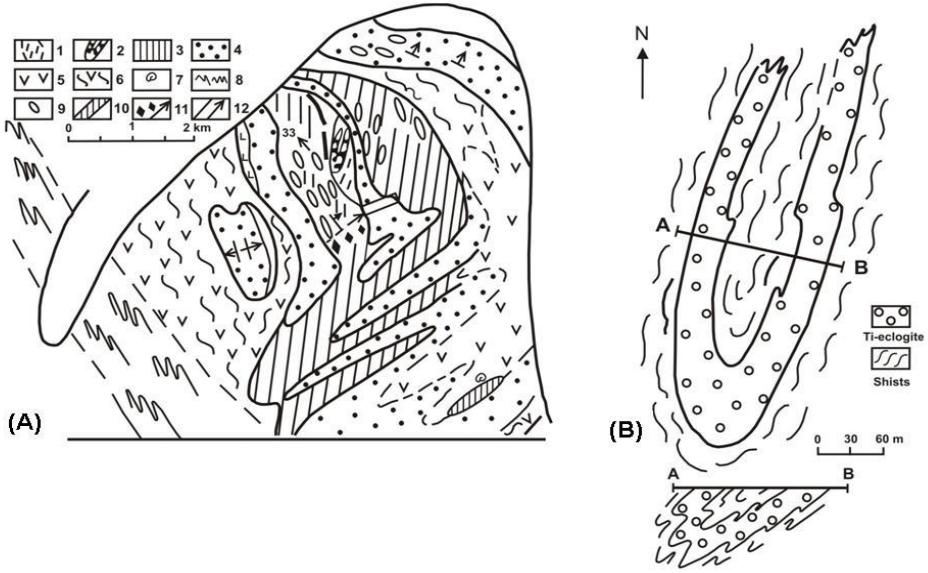
963 Localities for collecting representative samples of high-pressure rocks of the Maksyutov complex
964 and geological schemes of their outcrops



965

966

967 **Fig. 1.** Structural scheme of the Maksyutov complex (a) and detaile studied frame (b) (Lennykh and Valizer 1999). 1 –
968 Mesozoic and Kainozoic sediments, 2 – Zilair flysch (D_3-C_1), 3 – Silurian sediments and vulcanites, 4 – quartzite-schist
969 strata of the Suvanyak complex (Cm?), 5 – folded blastomylonites, 6 - the Second (ophiolitic) unit, 7 – the first
970 (eclogitic) unit of the Maksyutov complex, 8 – ultramafic rocks of the Khalilov massif, 9 – amphibolites, 10 -
971 serpentinites and serpentinitic melange, 11 – diabase dikes, 12 – Yantyshev-Yuluk thrust, 13 - tectonic contact



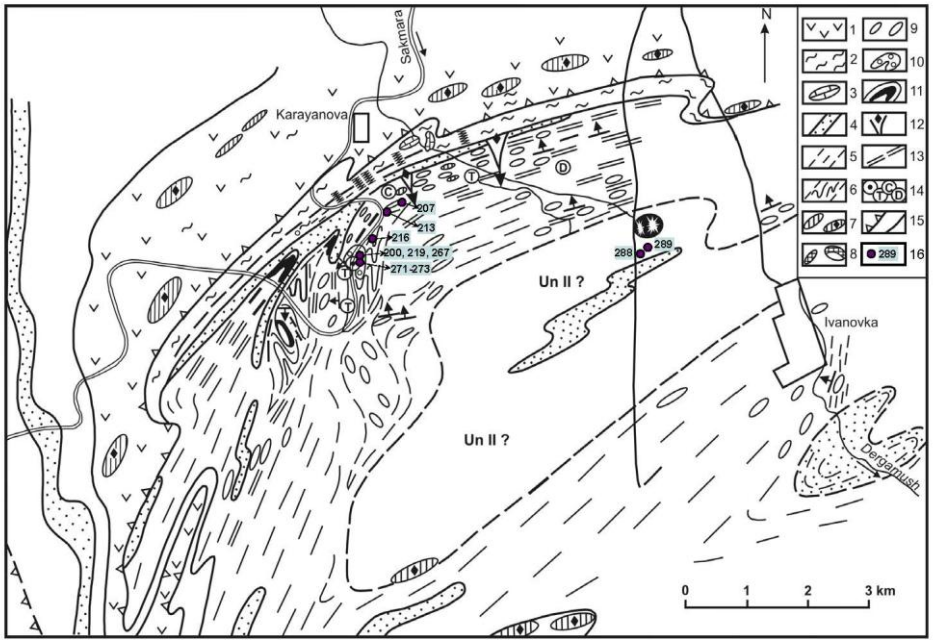
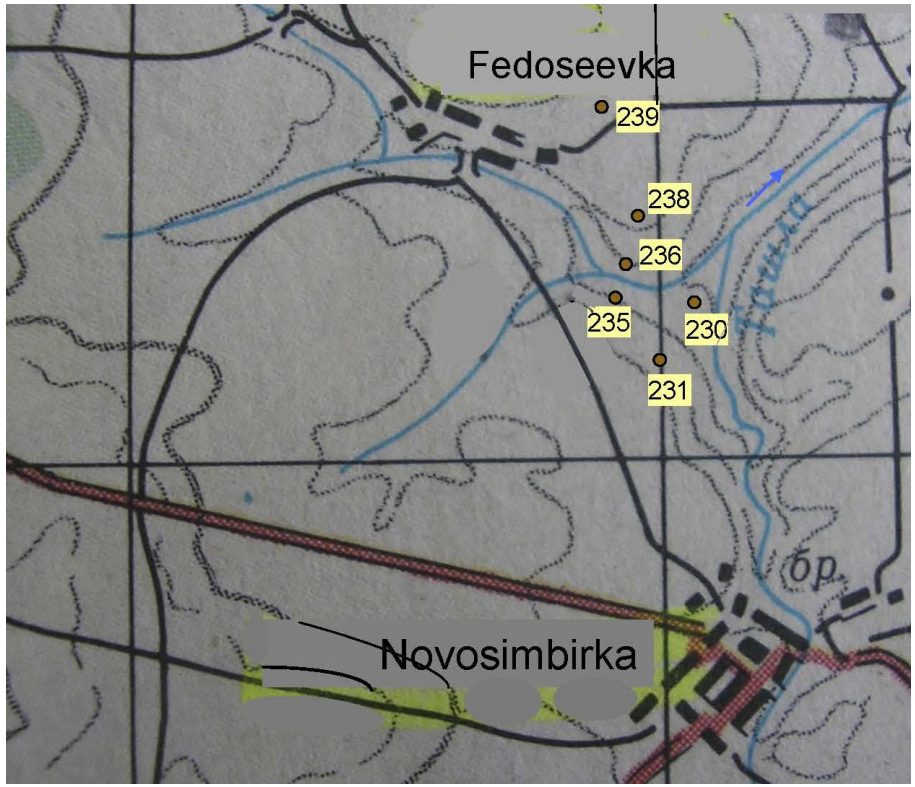


Fig. 2. A - Geological scheme of the southern part of the Maksyutov complex (location Shubino village (Lennykh and Valiser 1999). 1 – ancient structure and mineral associations, 2 – barroisite eclogites with rutile, 3 – lower “eclogite” subunit, 4 –

Fig. 3. Geological scheme and samples locality in Karayanova and Ivanovka areas (Lennykh 1999 with authors additions). 1-3 – the Upper unit, 1 – metavolcanites, 2 – metasediments, 3 – marbles, 4-6 – the Low unit^ 4 – yumaguzin sub-unit, 5 – eclogitic rocks, 6 – ancient eclogitic

Yumaguzin suite, 5 – volcanogenic part of the Second unit, 6 - the Second unit, 7 – marbles, - blastomylonite, 9 – eclogites, 10 – serpentinitic melange, 11 – diabases, 12 – elements of bedding of foliation; B – scheme of structure of the Shubino eclogitic body

rocks, 7 – serpentinites with Law rodingites, 8 – En rocks, 9 – eclogites, 10 – barroisite eclogites, 11 – fluid mineral formation in fold hinge, 12 – trend of disappearance of Law, 13 – shear zone, 14 - location of findings: A – graphite cuboids, B – Grt with pseudomorphs on coesite?, C – Tc-Phg association, D – Jd-Qz association. 15 – trusts and contacts, 16 – sampling points



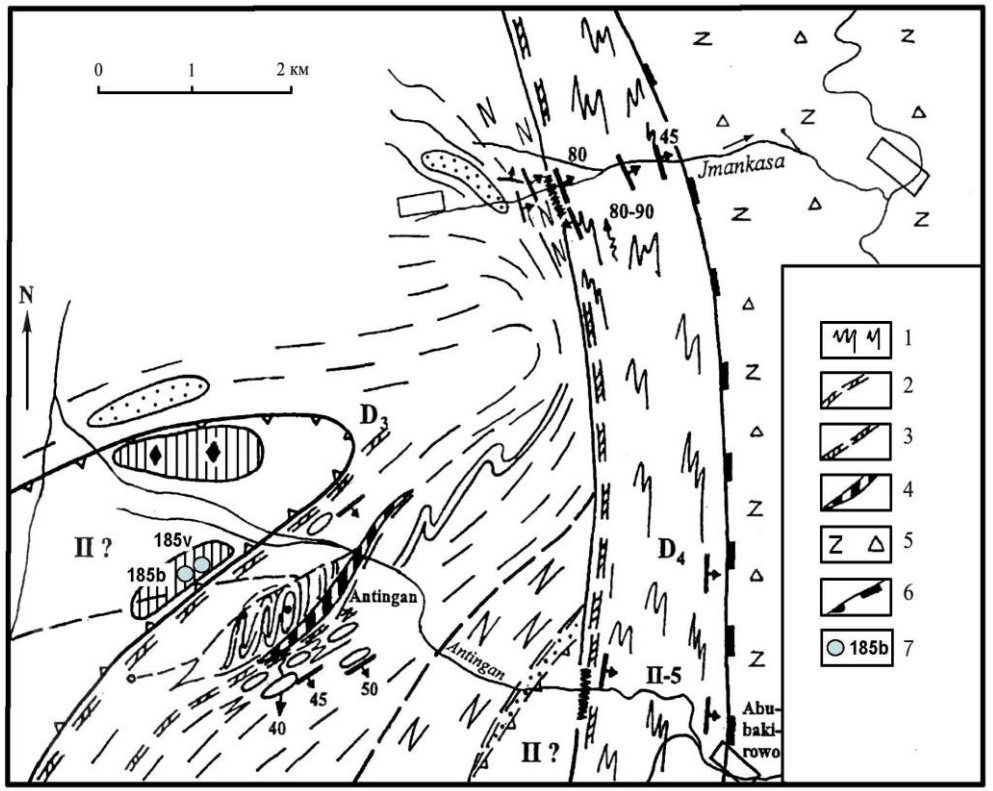


Fig. 4. Localities for collecting representative samples of high-pressure rocks in Novosimbirka (Fedoseevka) area

Fig. 5. Geological scheme of the locality of Antingan village (Lennykh 1999).1 – zone of the last blastomylonites (D_4), 2 – D_3 shear zone, 3 – D_4 shear zone, 4 - shear zone, with fluid mineral formation 5 – melange of the mail serpentinite belt, 6 - the Main Ural Fault (MUF), 7 – sample location

974 **Supplementary Materials 2 (SM-2)**

Table 1. Mineral associations of rocks of the Maksyutov complex and temperatures of their formation according to different geothermometers

Sample No.	Location	Rock	Mineral association	Formation temperature	
				*T (°C)	**T (°C)
88-16	Shubino	Grt-Cpx eclogite	Grt + Cpx + Gln + Act + Brz + Wnc + Ep + Ms + Rt + Qz	573-916	604-914
88-17	Shubino	Grt-Cpx eclogite	Grt + Cpx + Gln + Act + Brz + Wnc + Ep + Ms + Qz	784-813	778-821
154a	Shubino	Grt-Gln eclogite	Grt + Cpx + Gln + Amp + Ep + Ms + Chl + Qz + Ttn + Rt + Ab	426-558	457-610
158	Shubino	Grt-Gln schist	Grt + Cpx + Gln + Act + Ep + Ms + Chl + Qz + Ttn + Rt + Gr	537-604	563-747
159	Shubino	Grt-Gln eclogite	Grt + Cpx + Gln + Act + Ep + Ms + Chl + Rt + Qz	675-823	711-837
161	Shubino	Grt-Gln-Rt eclogite	Grt + Cpx + Gln + Amp + Ep + Ms + Chl + Qz + Ttn + Rt + Gr	680-751	767-788
163	Shubino	Grt-Ep-Act rock	Grt + Cpx + Gln +Act + Ep + Ms + Chl + Qz + Ttn + Rt	—	—
185v	Antingan	Alterated eclogite	Grt + Cpx + Gln + Amp + Ep + Ms + Qz + Ttn + Rt	406-553	447-595
200-1	Karayanovo	Grt-Gln eclogite	Grt + Cpx + Gln + Ms + Qz + Ttn + Rt + Opq	589-654	558-631
200-2	Karayanovo	Grt-Cpx eclogite	Grt + Cpx + Gln + Ms + Qz + Ttn + Rt + Opq	551-751	543-696
200-3	Karayanovo	Qz-Cpx-Gln interlayer	Qz + Cpx + Gln + Grt + Opq	527-510	494-718
207	Karayanovo	Grt-Gln eclogite	Grt + Cpx + Gln + Ep + Ms + Qz + Ttn + Rt	583-823	630-819
213	Karayanovo	Eclogite	Grt + Cpx + Gln + Act + Ms + Qz + Ttn + Rt	—	—
216	Karayanovo	Grt-Gln eclogite	Grt + Cpx + Gln + Act + Amp + Ep + Ms + Qz + Rt + Ab	613-669	638-688

219	Karayanovo	Alterated eclogite	Grt +Cpx + Gln + Act + Ms + Qz + Rt	644-718	690-737
230	Novosimbirka	Alterated eclogite	Grt + Cpx + Gln + Act + Ep + Czo + Rt + Chl + Qz + Ttn + Ab	483-530	513-564
231	Novosimbirka	Alterated eclogite	Grt + Cpx + Gln + Act + Ep + Chl + Qz + Ttn + Ab	606-673	596-705
235	Novosimbirka	Alterated	Grt + Cpx + Gln + Act + Ep + Chl + Qz + Ttn + Ab	468-554	500-608
236	Novosimbirka	Chl-Ep rock eclogite	Grt + Cpx + Act + Ep + Czo + Chl + Qz + Ttn + Rt + Opq + Ab	302-417	397-481
238	Novosimbirka	Grt-Gln schist	Grt + Gln + Act + Ep + Chl + Qz + Ttn + Rt + Opq + Ab	500-670	547-718
239	Novosimbirka	Grt-Ep-Amp rock	Grt + Cpx + Gln + Ep + Czo + Qz + Ttn + Rt + Ab	413-676	470-717
267	Karayanovo	Grt-Omp eclogite	Grt + Cpx + Gln + Ep + Qz + Ttn + Opq + Ab	570-771	591-784
271	Karayanovo	Grt-Gln-Omp eclogite	Grt + Cpx + Gln + Act + Amp + Ep + Ms + Chl + Qz + Rt + Cal	858-925	876-919
273	Karayanovo	Grt-Gln-Rt eclogite	Grt + Cpx + Gln + Act + Ms + Chl + Qz + Pl	516-725	523-761
288	Ivanovka	Grt-Gln schist	Grt + Cpx + Gln + Act + Ep + Ms + Chl + Qz + Ttn + Rt + Ab	445-508	504-566
289	Ivanovka	Grt-Act-Ep-Chl rock	Grt + Act + Ep + Ms + Chl + Qz + Ttn + Ab	544-930	571-916

Note: Mineral abbreviations are after Whitney and Evans (2010).

Temperatures calculated at P = 2.5 GPa according to: *Krogh Ravna (2000) and **Powell (1985).

Samples 88-16 and 88-17 were kindly donated by P.M. Valizer (Ilmeny State Reserve).

Table 2. Physicochemical condition of formation of HP rocks of the Maksyutov complex and their P-T trends

982

Sample No	Location	Temperature of formation from the Grt-Cpx equilibrium (Powell 1985), °C			Pressure, GPa		Temperature trend from core to rim of zoned grain, °C	Classification of P-T trend, T, °C
		Core, inclusions	Middle zone, inclusions	Rims and contacts	Petrological data	Pl-Cpx-Qz barometer (Perchuk 1992)		
88-16	Shubino	875	786	770-626	3.5-2.5		875-625	1й Retr. **875**-630
88-17	Shubino	805-830	849	881-892	3.5		805-890	1й Progr. **>800-900**
154a-pr	Shubino	448-511		518-620	1.5	1.19-1.26	450-620	3б Progr. 400-**630**
154a	Shubino	406-519		511-628	1.5	1.19-1.26	405-630	3б Progr. 400-**630**
158	Shubino	563-585		622-708	2.5		565-710	2й Progr. 560-**790**
159	Shubino	866-788		781-731	3.5		865-730	1й Retr. **875**-630
161	Shubino	801-816	802	892-899	3.5		800-900	1й Progr. **>800-900**
230B-1	Novosimbirka	544-459	509-433	385-313	1.0	1.19-1.17-1.04	545-315	4й Retr. 545-310
230B-2	Novosimbirka	493-498	528	545	1.0	1.11-1.16	495-545	4й Progr. 385-545
231	Novosimbirka	562-581	587	601-679	1.5	1.20-1.33	560-680	3a Progr. **470**-690
235	Novosimbirka	470-522	484-541	548-575	1.0	0.74-1.26	470-575	4й Progr. 385-545

236-1	Novosimbirka	384-419	372	423-453	1.0	0.96-1.16	385-455	4й Progr. 385-545
238-1	Novosimbirka	490	526	693	1.5		490-695	3а Progr. **470**-690
238-2	Novosimbirka	513	549	639-741	2.0		515-740	2й Progr. 560-**790**
238-2-2	Novosimbirka	665	690	817	2.5		665-815	1й Progr. **>800-900**
239-1	Novosimbirka	650	624	560	1.5	1.37-1.1	650-560	3й Retr. **690**-450
239-2	Novosimbirka	692-569	451	381	1.5	1.34-1.03	690-380	3й Retr. **690**-450
239-3	Novosimbirka	593-541	531	514-450	1.5	1.31-1.13	595-450	3-4й Retr.. **590**-450
185b-1	Antingan	473-496	517	526-657	1.5-2.0		475-655	3а Progr. **470**-690
185b-2	Antingan	594	573	546-498	1.5		595-500	4й Retr. 595-450
185v-1	Antingan	427-479	521	571-595	2.5		425-595	3б Progr.. 400-**630**

PT trends of deep inclusions: 800-890 °C – prograde, 875-720-625 °C – retrograde;

PT trends of subduction metamorphism: 470-710-740 °C – prograde, from 690-725 to 440-675 °C

End of Table 2

Sample No	Location	Temperature of formation from the Grt-Cpx equilibrium (Powell 1985), ºC	Pressure, GPa	Temperature trend from core	Classification of P-T trend, T, ºC

		Core, inclusions	Middle zone, inclusions	Rims and contacts	Petrological data	Pl-Cpx-Qz barometer (Perchuk 1992)	to rim of zoned grain, °C	
200-I c	Karayanovo	622-627		677-680	3.2		620-680	3а Progr.. **470**-690
200-II m	Karayanovo	619-637	677	770	3.2		620-770	2й Progr.. 560-**790**
200-III r	Karayanovo	744-704	691	673	3.2		745-675	2й Retr. 750-610
200-IV mx	Karayanovo	473-516	487	564-627	3.0		475-625	3б Progr.. 400-**630**
207-I-inn	Karayanovo	568	599-608	625-751	1.5	1.37-1.40	570-750	2й Progr.. 560-**790**
207-II-out	Karayanovo	689		789	1.5		690-790	2й Progr.. 560-**790**
207-III	Karayanovo	559	615-639	649-688	1.5		560-690	3а Progr.. **470**-690
216-inn	Karayanovo	727-694	715	663-613	1.5	1.43-(1.6)	725-615	2й Retr. 750-610
216-out	Karayanovo	629	631	635-658	1.5	(1.66)-1.46	630-660	3а Progr.. **470**-690
219	Karayanovo	591-597	676	766	3.0		590-765	2й Progr.. 560-**790**
219-2	Karayanovo	671	708-714	751	3.0		670-750	2й Progr.. 560-**790**
219-3	Karayanovo	544-580	694	773	3.0		545-775	2й Progr.. 560-**790**
219-3-1	Karayanovo	523-556	718	843	3.4		525-845	1й Progr.. **>800-900**
267-1	Karayanovo	591-598	646	726-784	2.6		590-785	2й Progr.. 560-**790**
267-2	Karayanovo	475-561	610	617-667	2.4		475-665	3а Progr.. **470**-690
267-2-pr	Karayanovo	463-488	486-508	566-605	2.0		465-605	3б Progr.. 400-**630**

271	Karayanovo	661	681-716	793-907	3.4		660-910	1й Progr.. **>800-900**
273	Karayanovo	534-545	574	700-776	3.0		535-775	2й Progr. 560-**790**
288	Ivanovka	464-485	586	520-670	1.5	1.04-1.42	465-670	3а Progr. **470**-690
289-1 r	Ivanovka	627-592	525	484-474	1.5		625-475	3й Retr. 690-470
289-2 c	Ivanovka	638		721	2.0		640-720	2й Progr. 560-790
289-3-1	Ivanovka	564	480	475-449	2.0	(1.04-1.14)	565-450	4й Retr. 590-450
289-4 m	Ivanovka	728	584	440	2.0	(1.30→1.08)	730-440	2-3й Retr. 745-450
289-4-1sg	Ivanovka	470-492	559-605	709	1.5		470-710	2й Progr. 560-**710**
289-5 c	Ivanovka	536	564	698-712	2.0		535-710	2й Progr. 560-**710**

Note: 1 - separate sections of the same sample are designated by numbers and letters, separated by a hyphen;

2 - designations: pr - profile, inn - inner grain zone, out - outer grain zone, sg - fine grain, c - central part of the sample, m - middle part, r - edge zone, Progr. - prograde P-T trend, Retr. - retrograde P-T trend.

Supplementary material 3 (SM-3)

Table 1. Bulk-rock XRF analyses of eclogites and Grt-Gl rocks, Maksyutov eclogite-blueschist complex

Sample	154	158	159	161	163	185	200	207	213	216	219	267	288	289	230/231	235/236	238/239	271/27
	D	D	E	E	E	E	D	E	E	E	E	E	D	E	D	E	E	D
SiO2	50,55	45,84	47,73	51,48	47,16	50,95	51,38	51,71	52,02	52,42	61,12	50,97	51,14	41,79	50,18	52,24	48,27	51,8
TiO2	1,372	2,241	2,628	3,495	4,712	3,947	2,068	1,324	0,840	2,200	1,189	2,656	1,286	2,968	1,890	1,072	3,690	0,88
Al2O3	16,05	15,49	14,26	12,10	12,95	12,65	12,93	16,04	14,16	14,84	13,43	14,10	16,16	14,70	14,01	12,64	13,31	14,2
Fe2O3																		
FeO*	11,28	13,53	16,26	14,12	17,14	14,10	14,24	11,30	9,46	13,56	6,29	12,68	10,65	15,61	11,35	9,02	15,37	11,2
MnO	0,140	0,294	0,246	0,182	0,269	0,214	0,300	0,189	0,255	0,260	0,064	0,181	0,190	0,406	0,178	0,139	0,269	0,19
MgO	7,66	7,95	6,72	6,88	5,31	5,97	8,12	6,87	6,58	6,29	3,62	6,05	6,06	7,28	6,74	9,04	5,98	8,7
CaO	9,02	9,91	7,91	7,38	9,13	8,01	5,36	5,68	9,40	7,24	6,09	9,27	9,38	12,39	10,39	9,80	9,52	7,0
Na2O	4,01	3,52	3,25	2,79	1,91	3,11	4,12	5,50	5,60	3,53	6,77	3,56	3,62	2,10	4,17	4,14	2,40	3,9
K2O	0,02	0,29	0,24	0,33	0,04	0,05	0,29	0,47	0,98	0,02	0,11	0,38	0,28	0,07	0,03	0,05	0,18	0,9
H2O- ign.loss																		
P2O5	0,161	0,139	0,254	0,191	0,510	0,146	0,119	0,102	0,793	0,132	0,868	0,381	0,116	0,363	0,084	0,300	0,471	0,1
Sum	100,26	99,20	99,50	98,97	99,13	99,15	98,92	99,19	100,1	100,5	99,55	100,2	98,88	97,66	99,02	98,44	99,45	99,2
Mg#	0,56	0,57	0,41	0,48	0,37	0,44	0,52	0,53	0,57	0,47	0,52	0,47	0,52	0,47	0,53	0,65	0,42	0,5
Ca#	0,55	0,61	0,57	0,60	0,73	0,59	0,42	0,36	0,48	0,53	0,33	0,59	0,59	0,52	0,58	0,57	0,49	0,5

Norm calculations of the rock composition

Sample	154	158	159	161	163	185	200	207	213	216	219	267	288	289	230/231	235/236	238/239	271/27
Q (S)	0,00	0,00	0,00	2,55	2,11	1,99	0,00	0,00	0,00	0,00	3,91	0,00	0,00	0,00	0,00	0,00	0,00	0,0
Or (KAS6)	0,12	1,73	1,43	1,97	0,24	0,30	1,73	2,80	5,77	0,12	0,66	2,24	1,67	0,42	0,18	0,30	1,07	5,3
Ab (NAS6)	33,80	18,95	27,61	23,83	16,28	26,51	35,20	41,78	30,16	29,69	58,06	30,02	30,94	8,77	31,34	35,54	20,39	33,9
An (CAS2)	25,64	25,78	23,70	19,70	26,85	20,56	16,08	17,81	11,72	24,44	6,01	21,29	27,29	31,17	19,59	15,99	25,12	18,4
Ne(NAS2)	0,00	5,98	0,00	0,00	0,00	0,00	0,00	2,76	9,17	0,00	0,00	0,00	0,00	5,09	2,31	0,00	0,00	0,0
Di wo(CS)	7,54	9,59	5,95	6,76	6,62	7,80	4,22	4,18	12,54	4,41	8,13	9,34	7,98	12,36	13,35	13,20	8,19	6,8

Di en(MS)	3,74	4,53	2,37	3,06	2,40	3,36	1,95	1,97	6,16	1,86	3,87	4,11	3,64	5,28	6,36	7,57	3,29	3,5
Di fs(FS)	3,65	4,94	3,65	3,64	4,36	4,44	2,23	2,16	6,15	2,57	4,15	5,21	4,27	7,10	6,80	5,03	4,97	3,1
Hy en(MS)	0,45	0,00	3,45	14,32	10,99	11,70	8,78	0,00	0,00	13,22	5,31	5,88	4,82	0,00	0,00	2,11	10,82	2,4
Hy fs(FS)	0,44	0,00	5,32	17,03	20,00	15,47	10,06	0,00	0,00	18,26	5,69	7,46	5,65	0,00	0,00	1,40	16,35	2,1
Ol fo(M2S)	10,44	10,85	7,75	0,00	0,00	0,00	6,85	10,75	7,15	0,40	0,00	3,58	4,80	9,35	7,46	9,30	0,64	11,2
Ol fa(F2S)	11,24	13,05	13,21	0,00	0,00	0,00	8,67	13,03	7,88	0,61	0,00	5,01	6,21	13,89	8,81	6,82	1,07	11,1
Mt(FF)	0,00	0,00	0,00	0,00	0,00	0,00	0,00	0,00	0,00	0,00	0,00	0,00	0,00	0,00	0,00	0,00	0,00	0,0
Il(FT)	2,60	4,29	5,02	6,71	9,03	7,55	3,97	2,53	1,59	4,16	2,29	5,03	2,47	5,76	3,63	2,07	7,05	1,6
Ap(CP)	0,35	0,31	0,56	0,42	1,12	0,32	0,26	0,22	1,72	0,28	1,92	0,83	0,26	0,81	0,19	0,67	1,03	0,2
Total	100,01	100,00	100,02	99,99	100,00	100,00	100,00	99,99	100,01	100,02	100,00	100,00	100,00	100,00	100,02	100,00	99,99	100,0

Unnormalized Trace Elements (ppm):

Sample	154	158	159	161	163	185	200	207	213	216	219	267	288	289	230/231	235/236	238/239	271/27
Ni	57	66	102	106	57	46	44	109	55	45	38	58	39	176	55	109	65	7
Cr	116	130	130	185	22	57	72	188	138	59	131	105	131	295	164	316	77	22
Sc	39	48	31	31	30	38	45	39	32	45	20	42	41	46	43	39	32	4
V	316	317	365	334	431	416	405	269	241	337	172	378	339	349	367	278	498	27
Ba	11	115	63	67	6	31	40	79	160	17	24	117	51	23	25	21	93	12
Rb	1	5	5	5	0	2	7	9	22	1	3	7	16	2	1	1	3	1
Sr	149	52	210	161	151	231	31	108	134	60	153	109	176	84	94	190	104	7
Zr	74	209	272	208	298	279	124	113	84	157	137	219	80	193	125	70	215	5
Y	27	70	44	30	44	46	45	28	24	35	25	39	34	46	42	13	35	1
Nb	4,3	6,1	14,4	17,2	32,1	23,0	2,3	7,0	6,3	11,0	9,3	13,6	2,3	17,1	4,5	4,8	20,4	2
Ga	19	18	21	20	22	18	18	16	19	16	19	18	17	17	17	15	22	1
Cu	30	71	53	51	105	46	73	62	33	126	33	258	49	87	37	61	58	6
Zn	107	133	143	144	142	107	106	101	103	101	85	92	95	354	87	109	137	9
Pb	4	2	6	2	2	9	4	5	3	3	5	4	4	1	5	10	3	
La	4	5	24	16	28	22	7	10	11	12	16	21	4	14	7	5	20	
Ce	14	24	66	40	67	62	15	21	34	27	52	52	18	42	16	9	47	1
Th	0	1	1	1	2	3	1	2	0	4	2	2	1	1	0	1	2	
Nd	11	21	43	29	42	41	12	13	28	15	38	34	12	26	16	9	34	1
U	1	2	3	0	3	3	2	0	2	1	1	2	1	0	1	0	1	

D - depleted; E - enriched

Suplementary Materials 3 (SM-3)

Table 2. Bulk-rock ICP-MS analyses of eclogitic rocks, the Maksyutov complex

Sample ID	154	158	159	161	163	185	200	207	213	216	219	267	288	289	230/231	235/236	238/239	271/27
	D	D	E	E	E	E	D	E	E	E	E	E	D	E	D	E	E	D
La ppm	4,38	7,89	25,01	14,55	25,18	24,14	3,09	11,55	10,90	8,99	16,95	20,74	4,48	16,09	6,11	3,58	18,52	4,2
Ce ppm	11,18	21,97	59,72	37,54	64,05	59,16	9,60	20,58	30,62	21,30	51,24	51,13	11,87	39,15	16,55	9,18	46,60	10,1
Pr ppm	1,80	3,62	8,62	5,66	9,04	8,50	1,73	3,04	4,92	2,85	7,37	7,27	1,97	5,65	2,68	1,37	6,80	1,5
Nd ppm	9,34	19,10	40,54	26,46	41,01	38,63	9,73	13,01	25,81	12,51	36,01	33,25	10,22	26,96	14,11	6,70	31,54	7,4
Sm ppm	3,21	6,93	10,69	7,19	10,50	9,67	3,94	3,45	7,65	3,89	11,21	8,61	3,63	7,95	4,82	2,01	8,34	2,3
Eu ppm	1,25	2,06	3,52	2,37	3,53	2,93	1,52	1,25	2,36	1,60	3,60	2,64	1,33	2,75	1,99	0,71	2,78	0,9
Gd ppm	4,22	9,49	10,62	7,25	10,57	9,24	6,19	4,38	6,52	6,70	8,07	7,45	4,93	9,10	6,68	2,38	8,34	3,0
Tb ppm	0,78	1,96	1,66	1,16	1,72	1,46	1,27	0,80	0,88	1,26	0,88	1,12	0,92	1,55	1,25	0,42	1,35	0,5
Dy ppm	5,01	13,41	9,54	6,68	9,94	8,93	8,53	5,11	4,85	7,15	4,84	7,35	6,27	9,55	8,08	2,59	7,77	3,5
Ho ppm	1,03	2,86	1,79	1,20	1,87	1,84	1,81	1,09	0,90	1,40	0,97	1,58	1,35	1,94	1,68	0,51	1,46	0,7
Er ppm	2,73	8,01	4,45	2,89	4,55	5,02	5,06	3,02	2,31	3,73	2,59	4,33	3,73	5,20	4,64	1,37	3,52	2,0
Tm ppm	0,40	1,17	0,57	0,38	0,59	0,70	0,75	0,45	0,32	0,52	0,37	0,62	0,55	0,73	0,68	0,19	0,46	0,2
Yb ppm	2,39	7,07	3,31	2,16	3,39	4,28	4,57	2,78	1,98	3,20	2,22	3,77	3,36	4,51	4,08	1,22	2,65	1,7
Lu ppm	0,37	1,09	0,47	0,30	0,50	0,64	0,71	0,44	0,32	0,49	0,33	0,60	0,53	0,71	0,61	0,19	0,38	0,2
Ba ppm	2	108	56	56	5	28	34	73	158	14	21	114	45	23	22	16	87	11
Th ppm	0,27	0,99	1,57	1,12	2,47	2,73	0,14	1,30	0,54	2,82	1,02	2,94	0,46	1,51	0,36	0,35	1,62	0,3
Nb ppm	2,94	5,39	13,11	15,35	31,37	22,01	1,82	6,85	5,38	10,24	8,94	13,54	1,69	17,10	4,09	4,40	20,84	2,1
Y ppm	25,53	71,10	43,89	28,31	45,38	46,05	45,67	27,48	23,90	35,00	24,88	39,56	33,85	47,37	42,57	12,24	35,70	18,4
Hf ppm	2,01	5,29	7,14	5,20	7,75	7,32	3,42	2,92	2,20	4,14	3,80	5,75	2,22	4,71	3,38	1,94	5,69	1,4
Ta ppm	0,19	0,44	1,09	1,08	2,13	1,50	0,16	0,47	0,32	0,56	0,61	1,00	0,13	1,12	0,28	0,31	1,43	0,1
U ppm	0,14	0,36	0,53	0,28	0,73	1,01	0,21	0,38	0,51	0,98	1,32	0,78	0,32	0,29	0,17	0,13	0,52	0,1
Pb ppm	4,15	1,58	4,40	2,33	8,01	9,13	4,17	5,79	3,37	3,83	5,32	3,27	3,79	1,55	4,64	8,51	2,81	2,8
Rb ppm	0,3	5,3	4,4	4,3	0,5	1,2	7,0	9,6	22,3	0,5	3,0	6,6	15,5	1,7	0,9	0,9	3,0	11

Cs ppm	0,02	0,44	0,27	0,27	0,02	0,09	0,61	0,64	1,06	0,04	0,18	0,26	0,56	0,08	0,04	0,02	0,17	0,6
Sr ppm	148	52	212	154	154	236	32	111	136	62	158	111	181	85	97	193	107	7
Sc ppm	36,9	46,9	32,5	27,4	28,8	37,5	46,3	37,5	31,5	44,7	19,0	40,2	40,5	45,6	42,3	37,9	32,5	41
Zr ppm	71	201	273	190	308	288	120	113	81	153	139	215	78	190	123	70	215	5
La/Ybn	1,236	0,754	5,098	4,551	5,015	3,810	0,456	2,806	3,721	1,899	5,149	3,712	0,900	2,409	1,011	1,987	4,722	1,61
Nb/Thn	1,454	0,729	1,125	1,838	1,710	1,085	1,802	0,707	1,342	0,489	1,173	0,618	0,498	1,518	1,506	1,679	1,727	0,74
Eu/Eu*	1	0,8	1	1	1	0,95	0,94	0,94	1	1	1,2	1	1	1	1,1	1	1	1
Sr/Sr*	1,1	0,2	0,3	0,37	0,22	0,36	0,27	0,42	0,38	0,27	0,3	0,2	1,3	0,2	0,5	1,8	0,2	0

Note: Data on the primitive mantle (Hoffman, 1988) were used when calculating of normalizing relations and of geochemical anomalies of Eu and Sr.
D - depleted compositions, E - enriched compositions

Supplementary materials 4 (SM-4)

Brief petrographic information of selected samples of the Maksyutov complex.

This appendix presents brief petrographic characteristics of the most characteristic and informative samples of high-pressure rocks from the Maksyutov complex: descriptions and micrographs of thin sections and microprobe preparations, brief results of P-T determinations of their formation parameters, their position, and role in the formation of the complex. Of the five studied MC sites, the most interesting for the purposes of this study are the titanium eclogite site near the village of Shubino and the site of the former village of Karayanovo, 35 km north of Shubino. These sites represent the most intensely metamorphosed parts of the Maksyutov complex, where the high-pressure index minerals diamond and coesite have been discovered and studied. According to our data, the maximum formation parameters of the titanium eclogites in the Shubino area reach temperatures of up to 890-900°C at a pressure of approximately 3.5 GPa. Similar parameters (T up to 846-910°C and P ~ 3.4 GPa) were recorded in the area of the village of Karayanovo (Table 2 in SM-2), which determines the heightened interest in these formations. Some samples from this collection are described below.

Shubino village location

Thin section 154a. Garnet-glaucophane eclogite.

The rock under microscope has porphyroblastic structure and nematoblastic matrix. Porphyroblasts are brownish - red garnet, a 1 - 2 mm the crystals are shaped rhombic dodecahedron. Some porphyroblasts in thin section elongated in the chain. Grains of garnet slightly fractured, some of them intergrowth by fine grains of quartz, epidote, and glaucophane. Garnet grains account for 20% of the rock. The main part of nematoblastic groundmass is folded by glaucophane (50%), pyroxene (20%), epidote (20%), quartz (5%), and a small amount of flakes of muscovite. Glaucophane is major mineral of matrix, pale lilac, elongated prismatic habit. Thin needles of glaucophane elongated along schistosity, flow around the garnet grains. There are elongated shape (110), and the cross-section with two cleavages under angle 58o. Glaucophane is mineral with weak pleochroism - blue to purple on Ng and colorless on Nm, biaxial negative, the angle c N about 6-9o. The size of elongated grains of glaucophane is up to 0.8 mm. Pale green pyroxene has weak pleochroism, short prismatic grain shape (100) and (110), and a section with two cleavage under angle of 90 °, optically positive, the 2V axial angle is 70°, the extinction angle with Ng 50º. The optical properties of pyroxene related him to omphacite. Epidotes in the main fabric of rocks are elongated grains size 0.2 - 0.8 mm. Yellowish epidote grains have high relief and variegated high order interference colors. Quartz represented by small transparent quartz grains and their aggregates. Quartz with muscovite often confined to porphyroblast garnet. Accessory minerals: rutile and sphene. Sphene - brown granular sometimes spear shape of grains in the center of which grains of rutile are preserved. Sphene grain size of 0.1 mm, and rutile – part of millimeter. There are also pure grains of rutile, mainly in garnet porphyroblasts. Rutile in the rock is only 1%, sphene as well.

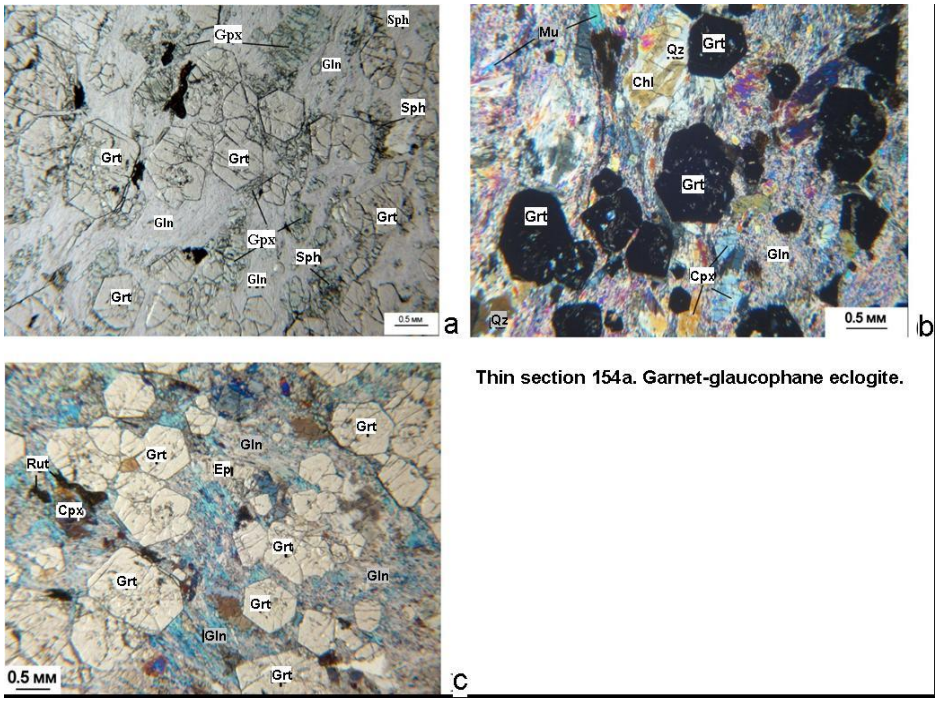


Fig. 1. Sample 154a Garnet-glaucophane eclogite (Shubino area), Microprobe profile of a newly formed garnet grain with progressive zoning (left). Parameters of formation (right): 3d cycle of prograde metamorphism: 405-630 ºC, 1,25 GPa.

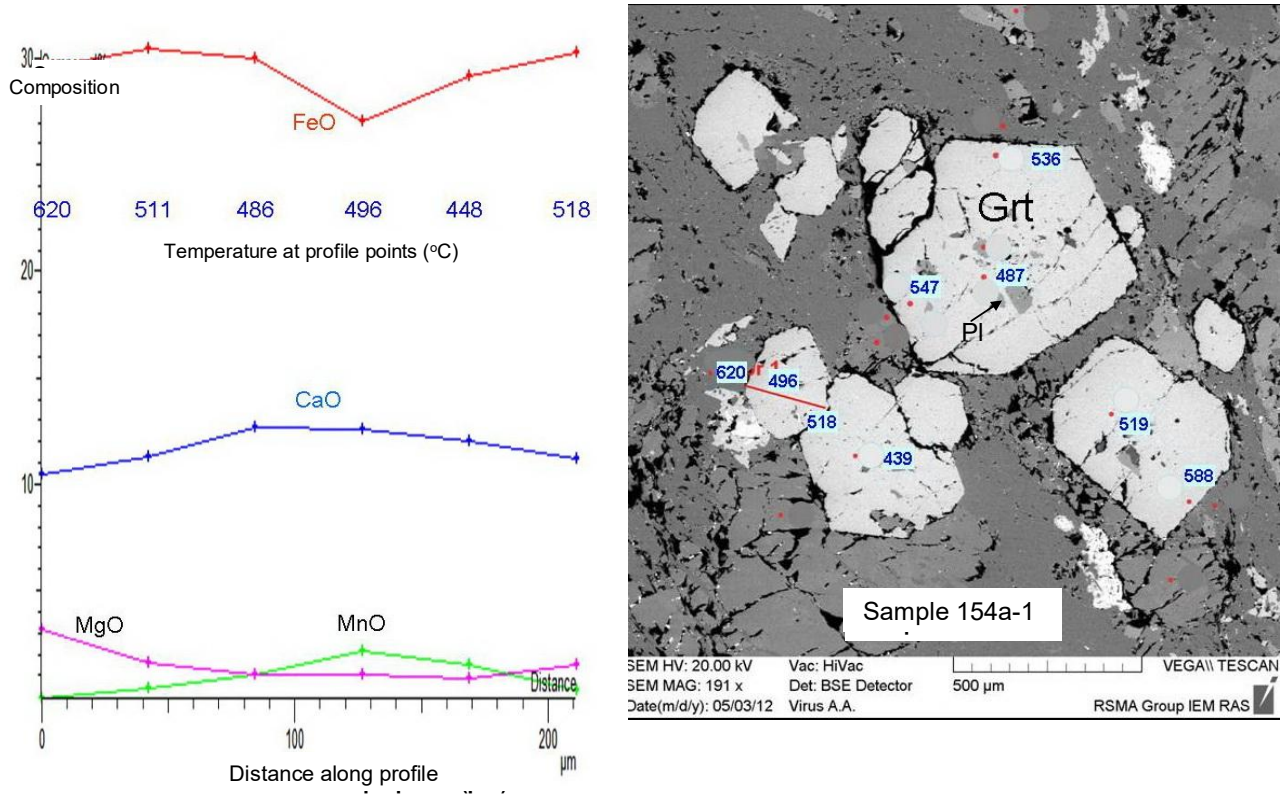


Fig. 2. Sample 154a-1. Progressive zoning of garnet in equilibrium with clinopyroxene records prograde conditions of the third stage of metamorphism (448-620 °C). Plagioclase inclusions in the center of the euhedral garnet grain reflect in their composition the pressure at the beginning of its crystallization - 1.19-1.26 GPa. The compositional profile of garnet in the newly formed grain repeats and intensifies the zoning up to 620 °C.

Thin section 159. Garnet-glaucophane eclogite

The rock under microscope has porphyroblastic structure, where large garnet porphyroblasts stand out from the matrix. They have brownish red color and crystalline appearance (rhombic dodecahedron), the size of 4-5 mm. Porphyroblasts of garnet are sprout by tiny minerals of groundmass: glaucophane, quartz, muscovite, epidote, chlorite, and very tiny grains of rutile. Garnet grains account for 30% of the rock volume. Base fabric of rock has nematoblastic structure; it composed of randomly arranged grains of bluish purple glaucophane (70%), pale green pyroxene (10%), epidote (10%), and rest of quartz, chlorite, muscovite, and accessory sphene and rutile. The glaucophane size grain of 0.4 - 0.6 mm. There are Gln sections extended to lengthen, and the cross section with two cleavages. Pale green pyroxene according to optical properties relate to omphacite. Omphacite grains are small size 0.2 - 0.4 mm, short prismatic habit, with a characteristic cross-sectional shape with two cleavages under angle of 89-90o, and extinction angle cN of about 70 degrees. Epidotes are rare elongated grains with characteristic colorful interference color, and size up to 0.6 mm. Generally, epidote grains are developing within of garnet porphyroblast rim together with lenses of quartz and muscovite flakes. Clean quartz grains are of mosaic image and size of 0.2 - 0.6 mm. They form lenses and layers within rim of garnet grains, like flakes of muscovite. Sphene is presented by brown granular grains with rutile inclusions in the center, because sphene is a decomposition product of rutile.

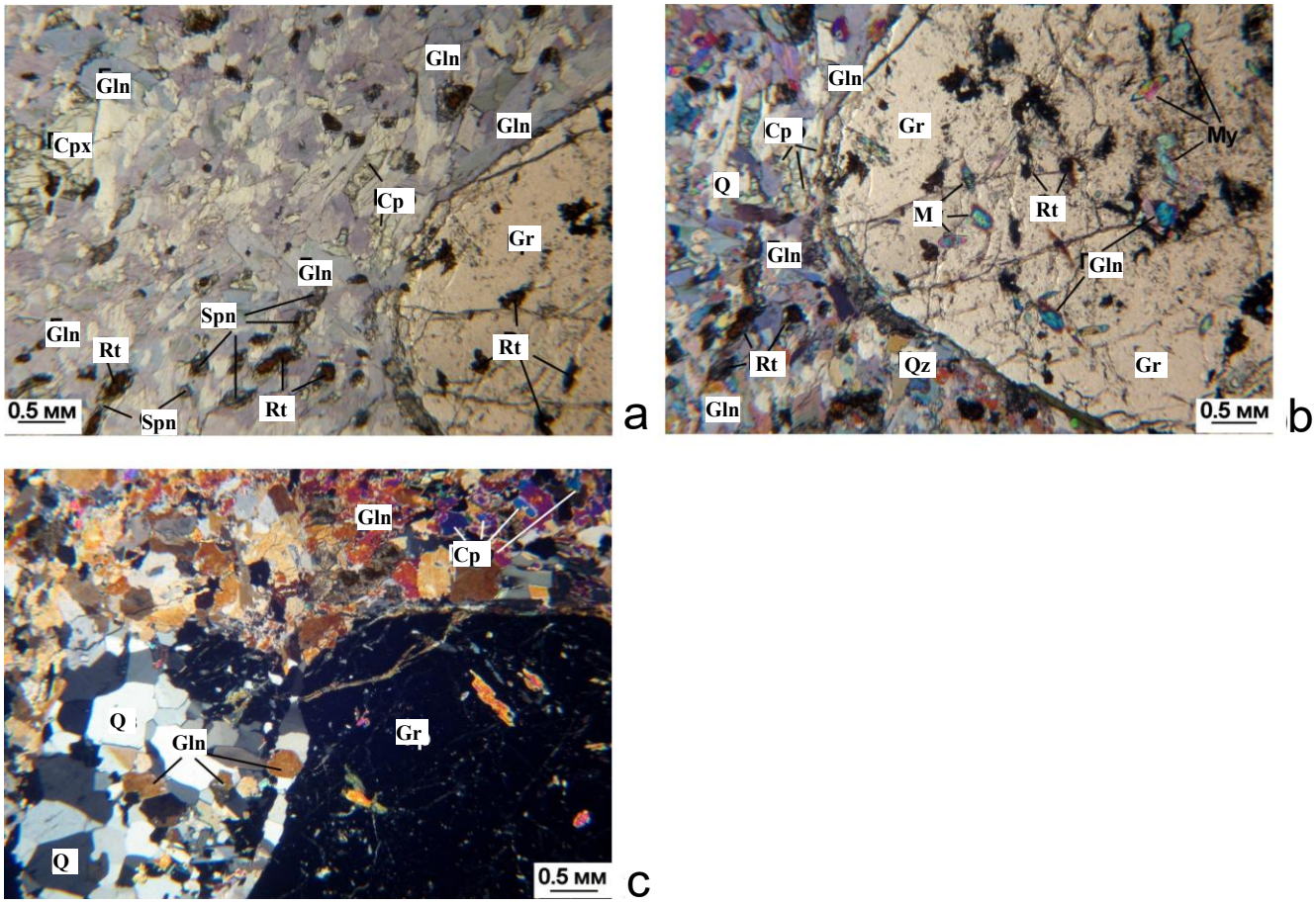


Fig. 3. Thin section 159 Garnet-glaucophane eclogite (Shubino area), Maximum retrograde trend for inclusion 865-730 ºC, 3,5 GPa. Rounded garnet grains highlight retrograde changes in composition.

Thin section 161. Glaucophane-garnet eclogite with rutile.

The rock has porphyroblastic structure, where porphyroblasts are brownish red garnet, a 3 - 4 mm, is 30%. Garnet grains of crystalline form, fractured. Quartz, chlorite, and muscovite are developing after them. There are quite broad rim of quartz grains with straight elongated facets and with flakes of muscovite around the garnet grains. Porphyroblasts garnet are filled by inclusions of minerals of rocks: glaucophane, epidote, muscovite, chlorite, sphene and small grains of rutile. Base fabric of rock is composed of pale green pyroxene - 40%, light purple glaucophane - 20% quartz - 20%, epidote - 10%, muscovite - 5%, rutile - 3%, chlorite - 2%, a small amount of plagioclase and sphene. The structure of the matrix is nematoblastic, it consist of prismatic grains of pyroxene, glaucophane, epidote. Pyroxene grains pale green, short prismatic habit. There are one or two (at an angle of 89o - 90o) cleavages in the different sections of the prism, which optically positive 2V - 70 degrees. Extinction angle CN - 49-50o. The optical properties relate to omphacite. The grain size of pyroxene 0.1 - 0.4 mm. Cpx on the edges of grains often replaced by violet blue glaucophane. Glaucophane - mineral prismatic shape, represent different sections in three directions: with one cleavage, with two cleavages (at an angle of 56 ° - 58o) and no cleavage. The grain size of glaucophane 0.1 - 0.5 mm. Glaucophane often replaces pyroxene on the edge of him grain. Quartz in rock is in the form of spots, lenses and rims around the garnet porphyroblasts. Pure grains of quartz have straight facets and size 0.1 - 0, 2 mm. Epidote are elongated grains prismatic shape with size 0.1 - 0.3 mm. Epidote germinate grains of garnet, pyroxene, and have high relief and variegated interference colors. Flakes of muscovite are random and are mainly associated with garnet porphyroblasts, range in size from a millimeter to 0.4 mm. Chlorite flakes of bright green, in the form of spots fusion of multiple grains with the size of 0.4 mm. These spots of chlorite associate with garnet. Accessory minerals in the rock are sphene and rutile. Sphene develops after porphyroblasts of garnet. Rutile has a significant amount in the rock; its small grains germinate in porphyroblasts of garnet. Rutile increases in size in the matrix, has a different cross-section: elongated and rounded. Rutile is characteristic mineral of eclogites of Shubino site. The grains of plagioclase (albite number 7) are present in the rock together with quartz and chlorite.

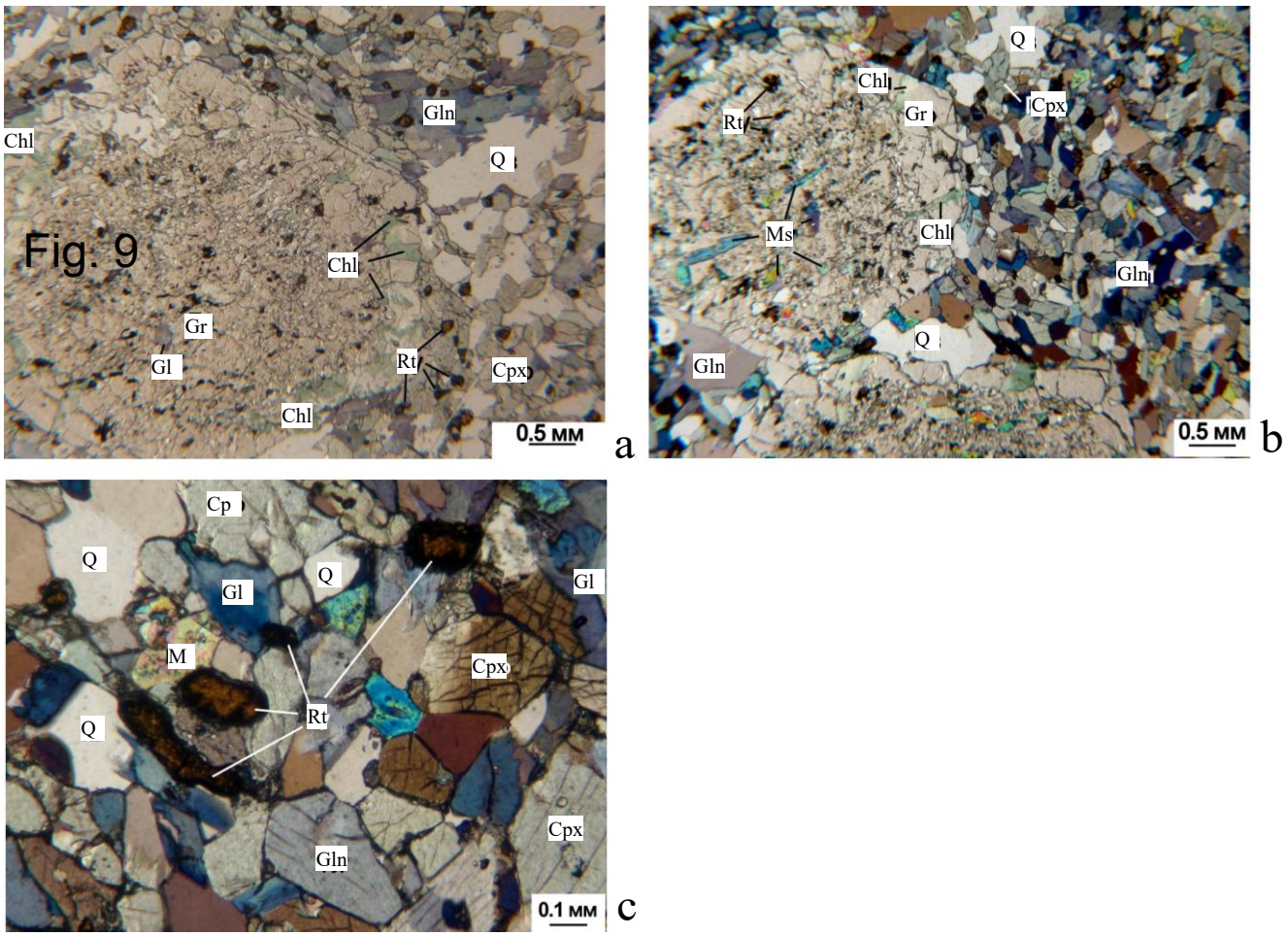


Fig. 4. Thin section 161. Glaucophane-garnet eclogite with rutile (Shubino area). Maximum prograde trend for deep ultramafic inclusion: 800-900 ºC, ~3,5 GPa. The richness of the rock with secondary minerals and rutile inclusions emphasizes the ancient age of the rock.

Sample 88-16 (Shubino location). Glaucophane-garnet eclogite with inclusions of quartz pseudomorphs after coesite?

In two titanium eclogite samples kindly provided to us by P.M. Valizer (Ilmensky State Nature Reserve), 88-16 and 88-17, garnet zoning recorded prograde and retrograde trends with maximum P-T parameters close to those in our samples 159 and 161. All four samples show maximum temperature trends (up to 890-900 °C), close to the coesite stability region, but never reaching it. One of the retrograde samples (88-16) retains traces of radial fracturing around quartz inclusions—presumable pseudomorphs after coesite. The garnets are strongly zoned, with a distinct, highly fractured, dark-red core containing abundant inclusions of rutile, clinozoisite, quartz, and possible quartz pseudomorphs after coesite; the broad, pale pinkish-orange rims are nearly free of inclusions. Below is a micrograph of garnet from this sample.

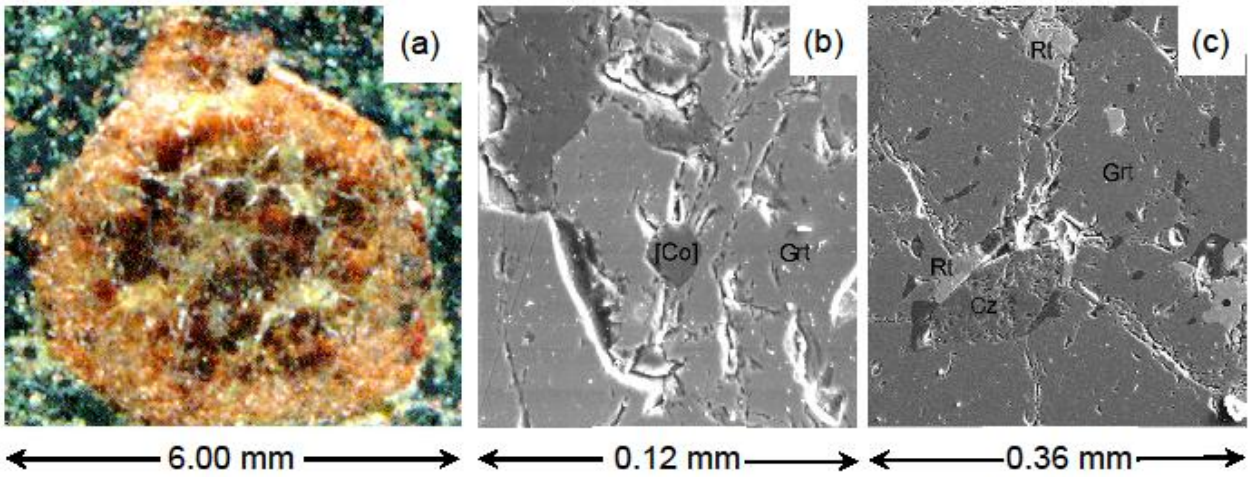


Fig. 5. Thin section 88-16 Microphotographs of garnet grains from a Ti-rich eclogite sample near Shubino, Unit #1: (**a**) zoned crystal with inclusions of quartz pseudomorphs after coesite? (**b**), inclusions of rutile, and (**c**) inclusions of clinozoisite. Retrograde garnet zoning trend: 875-625 ºC at P ~ 3.5 GPa.

Karayanovo former village location

Another important area for studying the conditions of formation and development of the tectonic-petrological model of the Maksyutovsky complex is the area of the former village of Karayanovo, which has been fairly well studied and is accessible to visitors. This area is distinguished by a great diversity of mineral assemblages and a wide range of parameters of their formation, from ultra-high results at T=845-910 oC and P~3.4 GPa to retrograde trends at T=745-615 oC and P~3.2-1.5 GPa. And yet, prograde tendencies of metamorphism (in 16 analyzed samples out of 18) prevail. At least three significant points of ultra-high-pressure bacterial mantle-crust and metasomatic inclusions are noted in this area: microdiamond inclusions in garnet (Bostic et al. 2003), ultramafic (Ol-En and En) inclusions (Valizer et al. 2013a), metasomatic ultramafic formations (Perchuk et al. 2024). Our observations also note high parameters of some educational associations, higher indicators of stability and coesite (Table 2 in Appendix 2).

Sample 271. Garnet-glaucophane-omphacite eclogite.

Grt-Gln-Omph eclogite was collected at the mouth of the left tributary of the Sakmara River among ultramafic (Ol-En) and eclogite rocks. The rocks of porphyroblastic structure composed of brownish red garnet porphyroblasts, grain size 1 - 2 mm. Garnet grains rarely retain crystalline form, are highly fragmented, with wide cracks filled with flakes of chlorite and muscovite. There are inclusions of small grains of rutile in the garnet crystals. Some grains of garnet in the center are completely filled with minerals of matrix: quartz, epidote, chlorite and muscovite. Garnet in the rock is 20%. Groundmass of rock has nematogranoblastic structure and consists of: pyroxene (40%), glaucophane (20%), quartz (7%), chlorite (7%), muscovite (5%), rutile (1%) as well as a small amount of sphene and calcite. Pyroxene is mineral of pale green, short - prismatic habit with specific sections one and two cleavages. The grain size of pyroxene is 0.2 - 0.6 mm. According to optical properties it related to omphacite. Rounded grains of quartz, muscovite flakes, elongated prisms of glaucophane and small grains of rutile develop over pyroxene. Glaucophane grains, size 0.1 - 0.8 mm have elongate prismatic habit. It has also a special zonal structure in this rock. The edges of the glaucophane grains have dark purple color, and the center of the grains bluish green, showing to difference in the composition of mineral. Quartz has isometric grains, size of 0.1 mm, occupies the space between the grains of

pyroxene, glaucophane, and garnet. Green chlorite develops around garnet, fused with muscovite and delimits grains of pyroxene. Particles of chlorite, size 0.4 mm. The calcite grains size of 1 mm presence together with chlorite at the fringes of the garnet grains. Small grains of glaucophane develop over calcite. Brownish grains of sphene, small spear-shaped and unformed mass involved grains of rutile. Fine grains and brownish red rutile inclusions present in garnet, pyroxene, muscovite, and glaucophane.

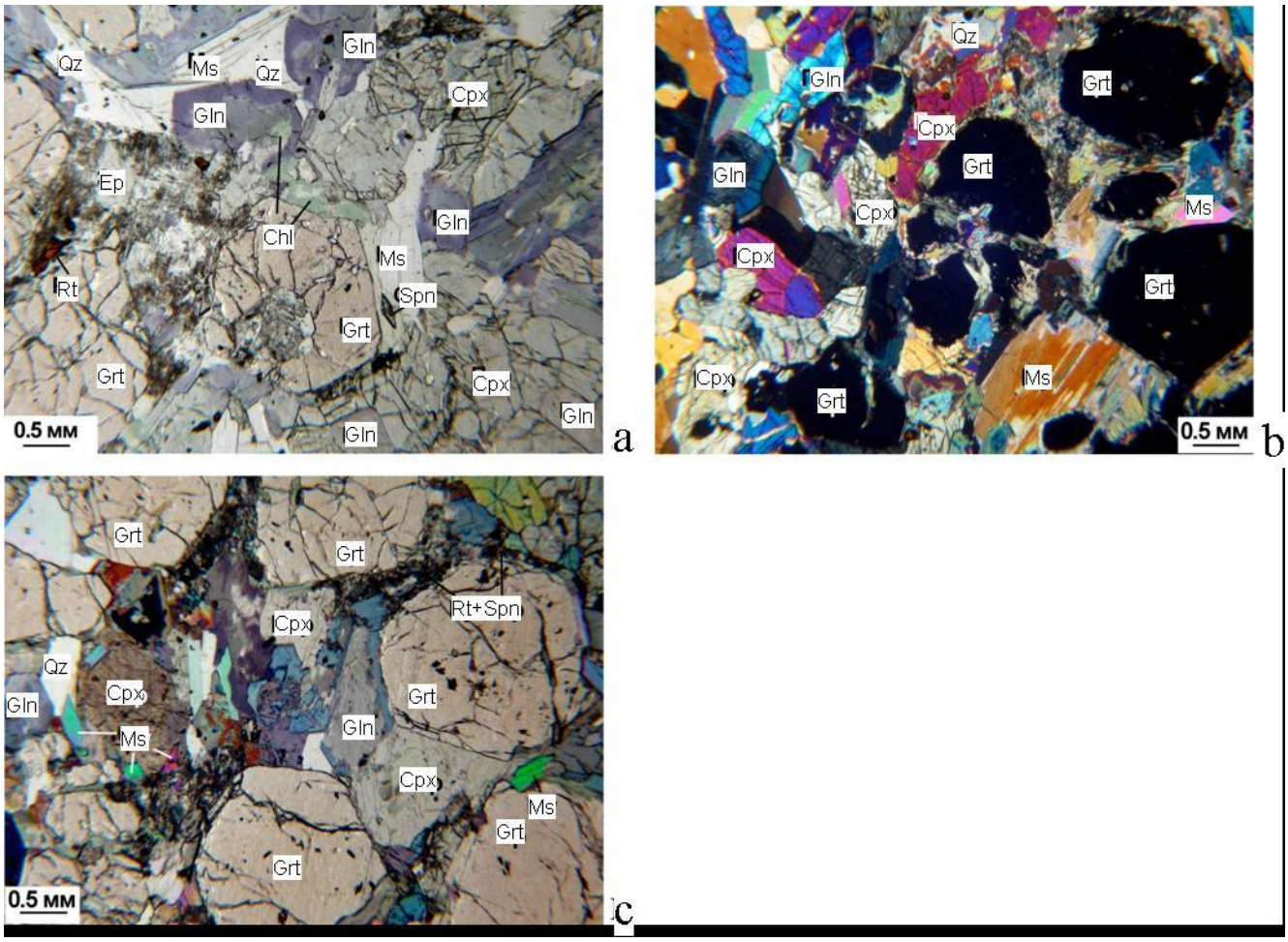


Fig. 6. Thin section 271. Garnet-glaucophane-omphacite eclogite (Karayanovo) area.

The sample contains a well-preserved Grt-Cpx association with a distinct prograde trend from 660 to 910°C. Plagioclase is absent from the rock, making it impossible to determine the pressure order.

Thin section 273. Garnet-glaucophane eclogite with rutile.

The rock of porphyroblastic structure where porphyroblasts brownish red garnet grains have a size of 2 - 5 mm. Garnet has crystal form. The cracks in the garnet are directed along of schistosity and filled with quartz and chlorite. Small grains of rutile are developed after garnet and directed across-the-schistosity. Garnet grains account for 30% of the rock volume. The main fabric has nematoblastic structure and composed of glaucophane elongate prismatic grains (50%), quartz (10%), chlorite (7%), rutile (2.5%), small amounts of actinolite and sphene. The main mineral in the rock is glaucophane of zonal structure that is seen in color: bright purple at edges and grayish blue at center of grains. Glaucophane has cleavage in two directions at an angle of 56 º - 58 º. Extinction angle CN is 9 º. Chlorite, actinolite, and rutile developed after glaucophane grains. Quartz grains have straight planes of the mosaic structure, size 0.1 mm, developed around garnet and in form of lens between the grains of glaucophane. Green chlorite, as quartz, develops at porphyroblast garnet rims. By interference

colors, gray yellow, chlorite refers to clinochlore. A characteristic feature of the rock is the significant content of rutile. Rutile grain brown red has elongated and rounded images. The large grains of rutile are developing after minerals of groundmass.

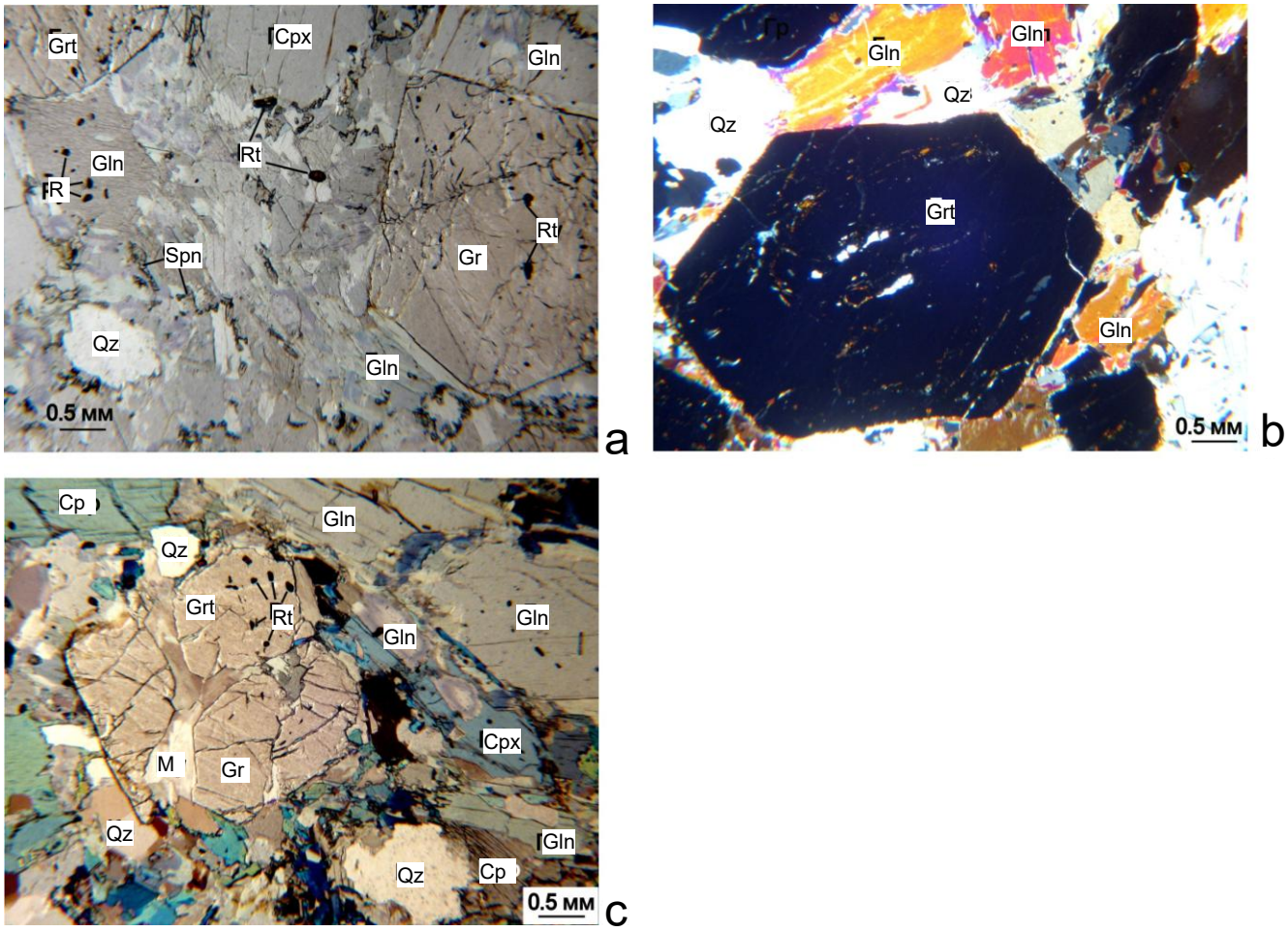


Fig. 7. Thin section 273. Garnet-glaucophane eclogite with rutile.

Rock of the 2nd prograde cycle: 535-775 ºC, ~3.0 GPa. The P-T parameters of its formation determine the maximum level of prograde metamorphism caused by the subduction of the complex. The difference in the maximum formation temperatures of these rocks (approximately 135 ºC) prevents these samples from being classified as products of a single metamorphic cycle.

Sample 216. Garnet-Glaucophane eclogite with rutile.

The rock shows porphyroblastic structure where the porphyroblasts of garnet of 3 - 4 mm have a crystal form (rhombic dodecahedron). Garnet grains are fractured and filled with quartz, glaucophane, muscovite and tiny grains of rutile. In some garnet grains the edge are preserved only, and the center of them are filled with matrix minerals. Garnet grains account for 20% of the rock. Base fabric of rocks consists of pale green pyroxene (55%), pale purple glaucophane (30%), quartz (10%), muscovite (3%) and rutile (2%). Grains of pyroxene are size of 0.1 - 0.4 mm, of pale green color, and short prismatic habit. The cross sections of the pyroxene grains have either one or two cleavages under 90 degree. By pyroxene the glaucophane develops. Glaucophane has elongated prismatic habit, with pleochroism pale violet by Ng and colorless by Np. Grain size of glaucophane up to 0.6 mm. Fine grains of quartz, of mosaic structure in the form of lenses and layers, are confined to porphyroblast of garnet. A characteristic feature of the rock is a significant amount of rutile. The grain size of rutile in the

groundmass is increased to 0.2 mm. Rutile grains brownish red in color with noticeable striation. Occasionally here are geniculated twins.

The sample is distinguished by its inversional zoning. The interior of the large grain displays retrograde zoning from 725 to 615°C at P = 1.43-1.6 GPa, while the overgrown outer zone, on the contrary, records a prograde compositional change in the range of 630-660°C at the same pressure (1.46 GPa). Evidence of retrograde alteration of the central part is clearly visible in the replacement of garnet by matrix minerals: pyroxene, glaucophane, quartz, rutile, and muscovite. Based on the temperature range, these changes in mineral composition are attributed to the second regressive stage of metamorphism. A return to the prograde stage of crystallization is very characteristic of rocks of the Maksyutov complex.

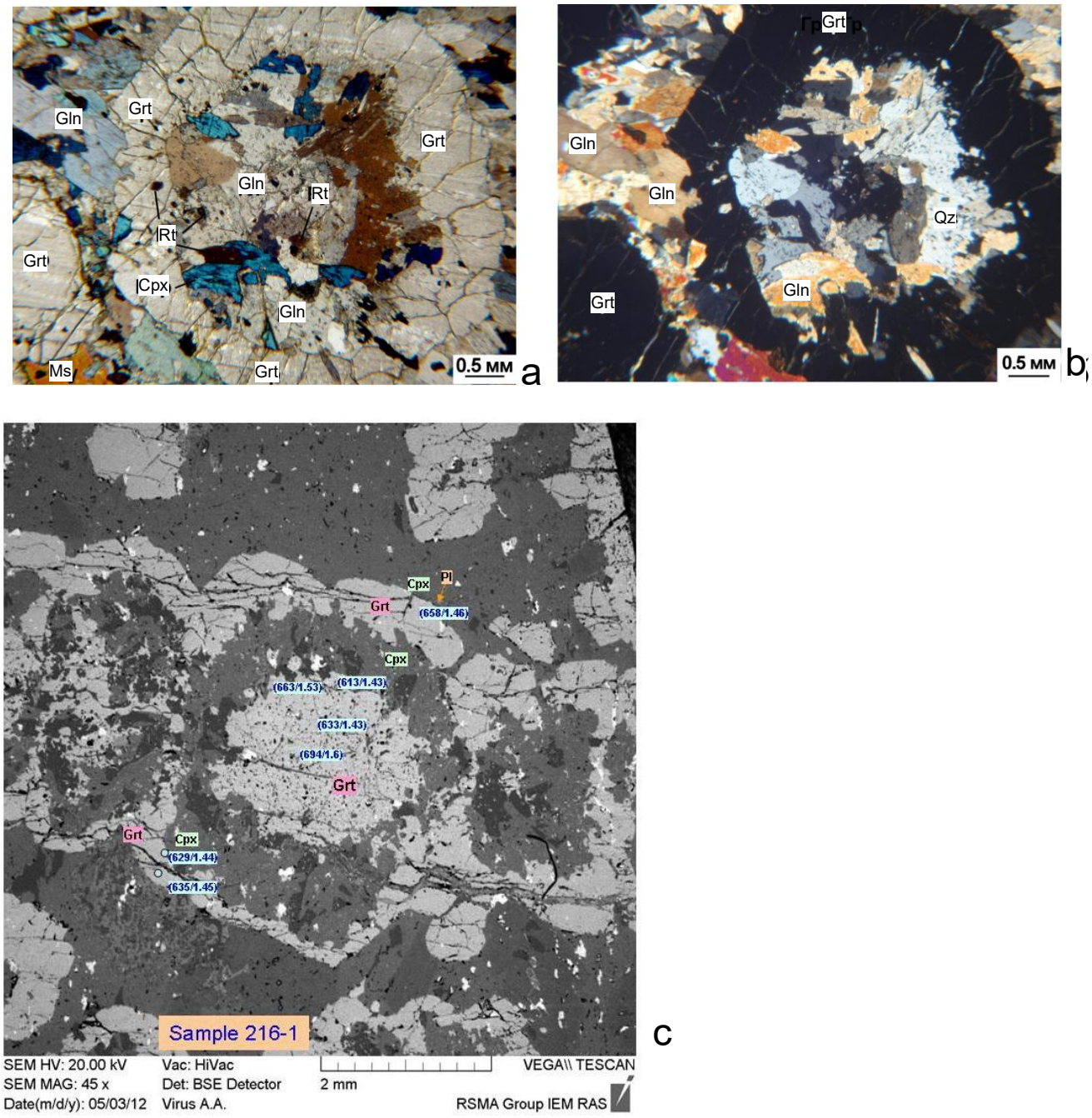


Fig. 8. Sample 216-1. (a)-(b) Contrasting inversion zoning of garnet in eclogites of the Maksyutov complex at the stage of coherent development (Sample 216-1, Karayanovo site): regressive - in the grain center 725 °C/1.6 GPa → 615 °C/1.4 GPa – Second regression cycle, and slightly progressive at

the margins 630 °C/1.44 GPa → 660 °C/1.46 GPa – 3d prograde cycle. (c) Microprobe thin section with points of study and calculated P-T parameters

Thin section 267. Garnet-omphacite eclogite with rutile.

The rock of porphyroblastic structure, where porphyroblasts of brownish red garnet, by crystalline habit, size 2 - 4 mm, in the form of interrupted chains. The garnet grains are fractured and the cracks are filled by quartz grains, muscovite, glaucophane, and tiny grains of rutile. Quartz with mosaic structure and straight facets, flakes of muscovite and chlorite are formed around the garnet grains. Garnet in the rock is up to 20%. Base fabric is represented by: pyroxene (50%), quartz (15%), glaucophane (5%), chlorite (5%), muscovite (3%), and rutile (2%). The pyroxene grains are pale green, up to 1 mm, fused with each other and with the garnet porphyroblasts. Quartz and muscovite occur between the grains of pyroxene. Typical sections with cleavage (110) at a right angle characterized for pyroxene. There are twins at the (100) plane. Pyroxene is optically positive with axial angle 2V - 70, the extinction angle 47 ^{0} -50 ^{0}. According to optical properties, pyroxene is classified as omphacite. Rounded grains of quartz, purple glaucophane, chlorite, and rutile are developed after grains of pyroxene. Grains of quartz, size 0.1 - 0.3 mm, confined to the garnet porphyroblasts, but there are small lenses of quartz between grains of pyroxene. Glaucophane has a purple color and marked pleochroism from dark - purple by Ng to colorless by Np. Small grains of glaucophane are formed after garnet and pyroxene. On the edge of the thin section there is gradational contact of garnet-omphacite eclogite and garnet-glaucophane schist. The glaucophane grains become elongated prismatic habit and elongated along with foliation. The grain size of glaucophane reaches 0.2 mm. Single grains of calcite observed in quartz-chlorite-glaucophane lens. Green chlorite flakes mainly developed in the garnet rims, as pyroxene. Muscovite and chlorite are developing after garnet grains and its intergrowth with quartz developed around of garnet and pyroxene. Particle size of muscovite is from a millimeter to 0.2 mm. A characteristic feature of the rock is a noticeable number of grains of rutile. He develops after all minerals of rock and has a grain size from a fraction of a millimeter to 0.1 mm. The larger grains of rutile, brownish red in color with striations confined to the lenses of quartz.

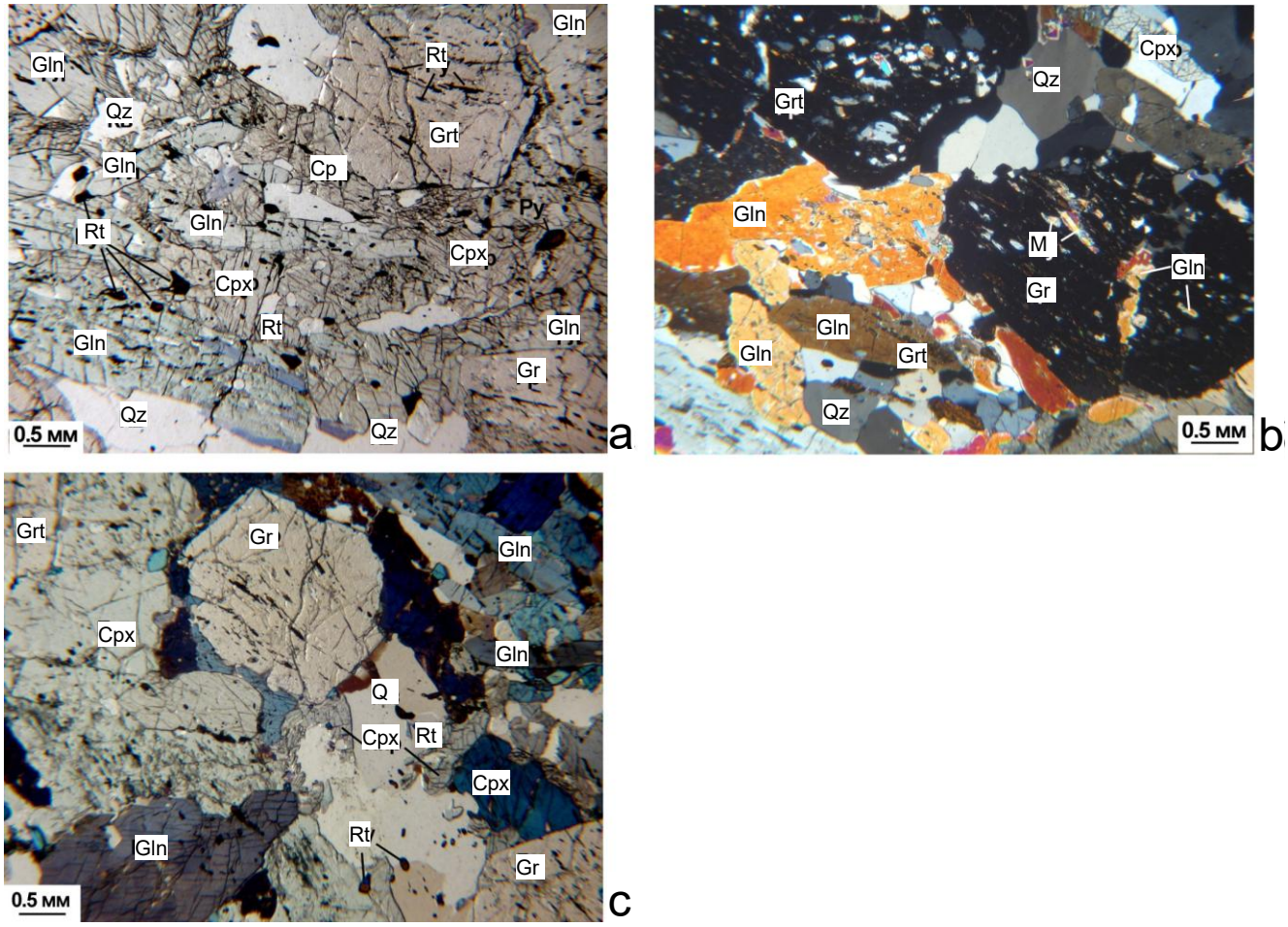


Fig. 9. Sample 267 (Karayanovo area). 3d prograde cycle of regional metamorphism 400-630 ºC/2,0 GPa according to mineral geothermobarometry. 650 ºC/2,3 GPa according to "Perplex" calculations.

Rare occurrences of radial fractures around quartz inclusions in garnet, omphacite, and glaucophane, interpreted as coesite pseudomorphs, and microdiamond aggregates in garnet identified by Raman spectroscopy, suggest that parts of the Maksyutov complex were subducted under SVD conditions (>2.8 GPa for coesite and >3.0 GPa for diamond at 600 °C) in the Late Devonian (385 Ma). To more accurately determine the petrotectonic evolution of the Maksyutov complex, we constructed isochemical phase equilibrium diagrams (pseudosections) for several representative metabasites in the NCKFMASHTO system based on bulk composition and effective volume data (Fig. 4). Data obtained using conventional thermobarometry and phase equilibrium modeling indicate higher peak equilibrium temperatures than previously reported. Isochemical phase diagrams indicate minimum conditions for prograde metamorphism: P-T 650-675°C and 2.4-2.6 GPa, while conventional thermobarometry records peak temperature conditions along the path of retrograde exhumation of the complex. However, even these peak pressure parameters turned out to be significantly lower than those required for the stability of coesite and diamond. Thus, ultra-high pressure (UHP) conditions were not achieved during the subduction of the Maksyutov complex.

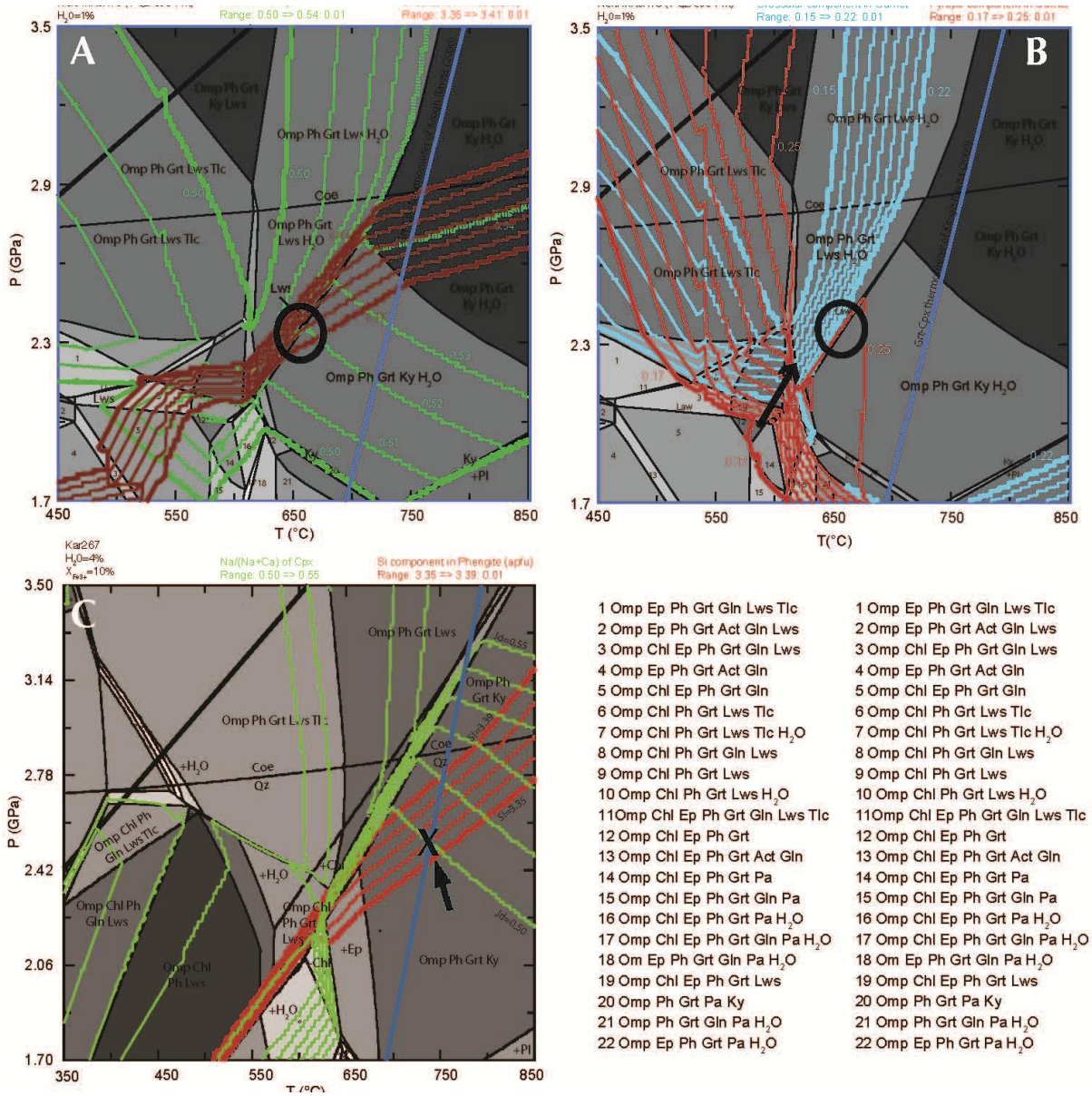


Fig. 10. Pseudo-section of the NCKFMASHTO system for sample 267 (Karayanovo region) of the Maksyutov complex for different compositions of omphacite and phengite (a), Ca and Mg in garnet (b) and water content from 1 % (b) to 4 % (c). X marks our best estimate of peak P-T conditions near, but not within, the coesite stability field at ~725 °C and 2.5 GPa (Fedkin et al, 2020)

Antingan site.

Intermediate section between the villages of Novosimbirka and Ivanovka (SM-1, Fig. 5). In the zone of the D3 and D4 sludge faults and the subsequent blastomylonite zone, 1.5 km west of the village of Antingan, isolated blocks of Grt-Gln eclogites are exposed. The samples collected include relatively fresh and altered eclogites.

Thin section 185b. Garnet-glaucophane eclogite.

Rock porphyroblastic structure where porphyroblasts are brownish red garnet grains of crystalline shape up to 3 mm. Garnet grains are fractured and are filled by inclusions of small grains of quartz, muscovite, glaucophane, epidote, chlorite, and tiny grains of rutile. Because of the wide cracks in the

garnet grains, it seems that garnet pilfered and rotated. Quartz, muscovite and glaucophane developed thru the cracks. Garnet grains account for 20% of the rock volume. Base fabric nematoblastic structure represented by: glaucophane (75%), epidote (10%), quartz (10%), muscovite (3%) and sphene (2%), rutile and chlorite less than 1%. Glaucophane has blue-lilac color, elongated prismatic shape, grain size 0.2 - 0.8 mm. Glaucophane grains flow around porphyroblasts of garnet grains and grows together with epidote. Epidote grains, prismatic shape, ranging in size from 0.2 mm to 0.6 mm, yellowish-white, have high relief and variegated interference color. Quartz represented by small transparent grains of 0.1 mm. It forms accumulations around garnet grains, streams and lenses in the main fabric of the rock. Accessory minerals are rutile and sphene. Sphene brown, shapeless and granular, grain size up to 0.2 mm curved according to schistosity rock. Sometimes in the middle of sphene grains remain small grains of rutile. Sphene is a product change of rutile.

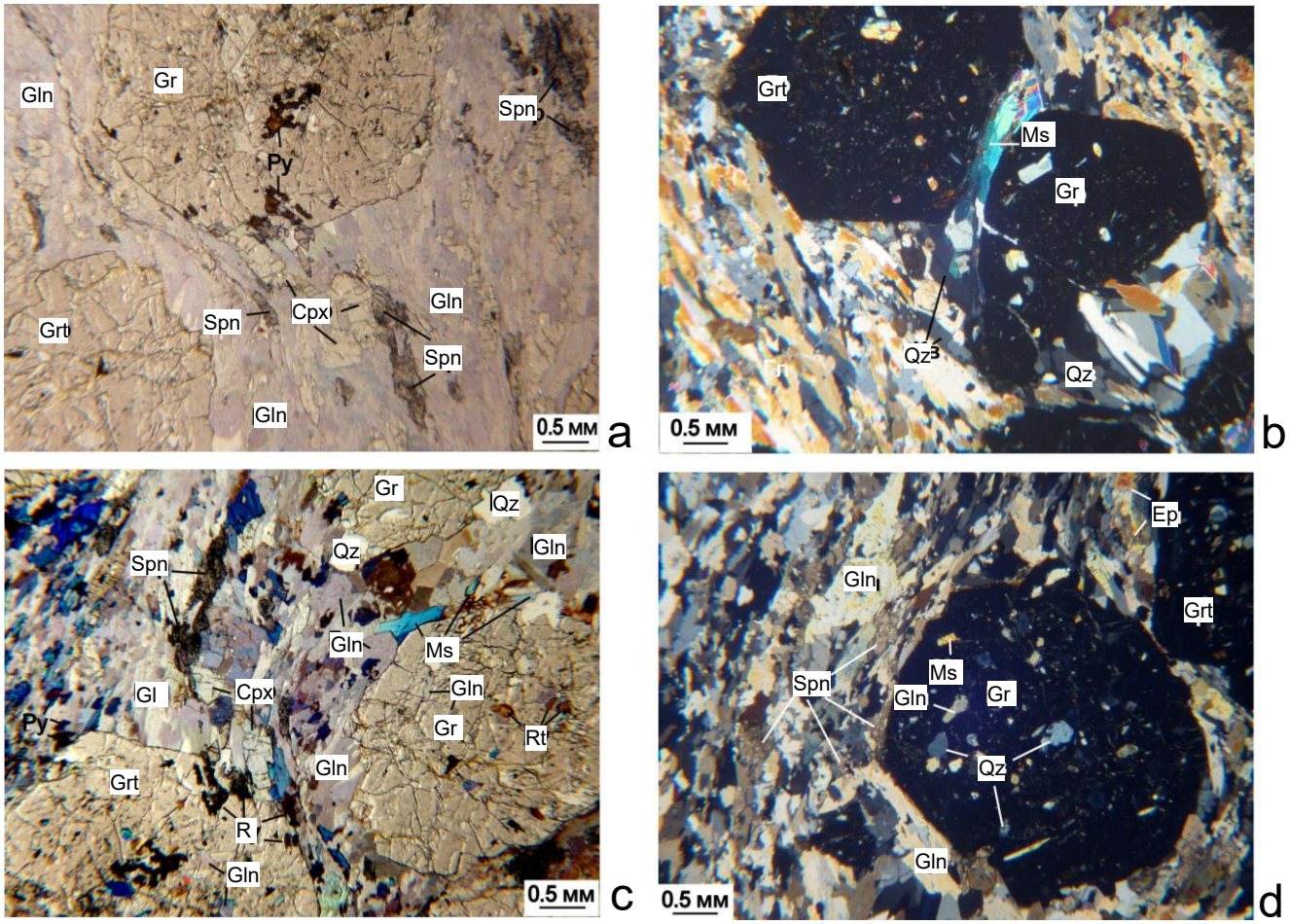


Fig. 11. Thin section 185b. Garnet-glaucophane eclogite in transmitted and polarized light.

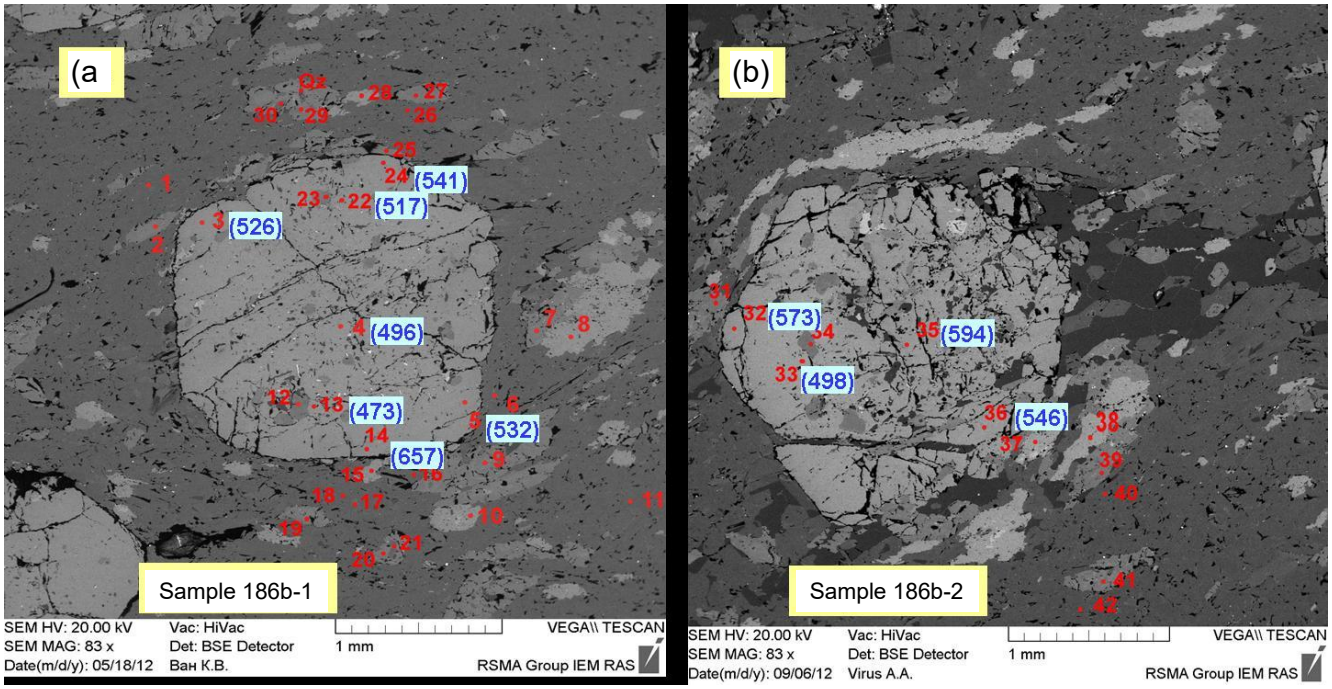


Fig. 12. Prograde (a) and retrograde (b) zoning of garnet in Grt-Gln eclogite from the Antingan site. Numbers indicate the analysis number; Grt-Cpx equilibrium temperature in parentheses is in °C.

It is significant that a number of samples exhibit double zoning of garnet grains (Fig. 4). Moreover, prograde P-T trends transition to retrograde ones within the same temperature range as the former (compare samples 185v-1 and 185b-2 in Table 2 of Appendix 2). This may indicate that the change in the direction of the metamorphic regime occurred almost instantaneously, which is unusual for conventional subduction metamorphism. Samples with prograde zoning of the grain are typically heavily altered by a subsequent retrograde (or second prograde) cycle, which determines the sequence of prograde-retrograde alterations.

Thin section 185v. Altered garnet-glaucophane eclogite.

Rock has porphyroblastic structure, which is represented by garnet, brownish red in color, size 3 - 4 mm. Garnet grains are strongly fractured and are filled by minerals presented in the rock: rounded quartz grains, prisms of glaucophane and epidote, muscovite flakes and tiny grains of rutile. Porphyroblasts of garnet are surrounded by grains of quartz with mosaic structure and by flakes of muscovite. Garnet is 20% of the rock volume. Matrix has nematoblastic structure and represent by glaucophane (60%), quartz (25%), epidote (15%), sphene (4%), rutile, and muscovite less then 1%. Glaucophane grains prismatic shape, size 0.1 - 0.3 mm elongated along the schistosity. Glaucophane grains have pleochroism from pale violet on Ng, to blue on Nm, and to yellowish on Np. Extinction angle CNg 9o, some grains have the extinction angle 22o, it speaks of the development of green amphibole after the glaucophane. Epidote yellowish brown, prismatic habit is presented in the rock, as isolated grains, and as intergrowth of a few grains together. The grains size of epidote from 0.1 to 0.4 mm. Quartz in the main fabric in the form of irregular flattened along schistosity grain size 0.1 - 0.2 mm. A characteristic feature of this rock is a significant amount of sphene. Sphene grains brown color, granular appearance, developing on all minerals of groundmass. Within the grains of sphene small grains of rutile are stored. According to the description of thin sections 185b and 185v rocks are similar, the only difference in the quantitative composition of minerals and grain size.

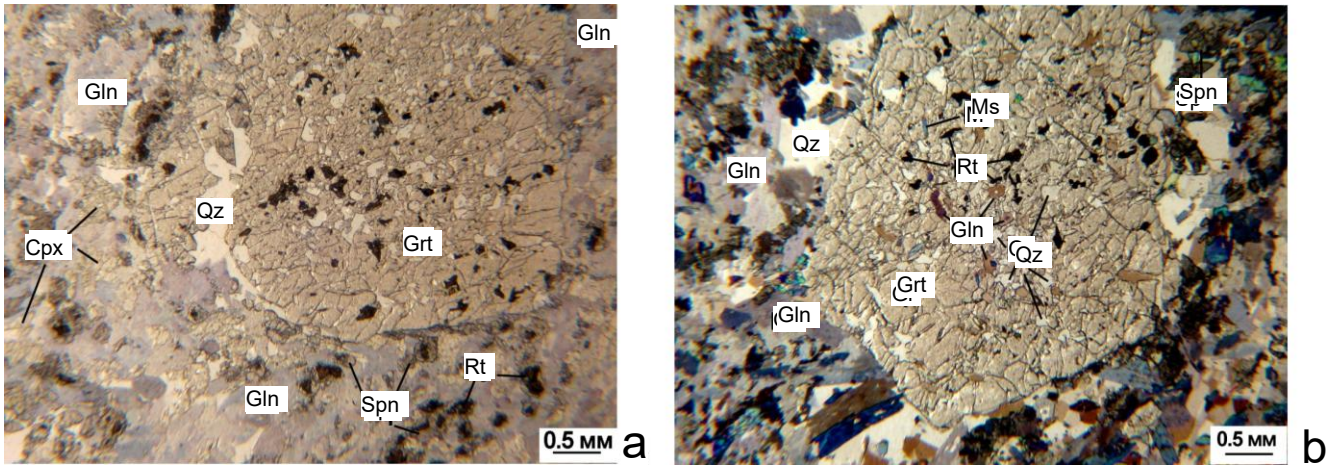


Fig. 13. Thin section 185v. Altered garnet-glaucophane eclogite with prograde zoning of garnet 425-595 ºC and 2,5 GPa (3d prograde cycle)

Novosimbirka village location.

Thin section 230 (Novosimbirka area). Garnet-epidote-glaucophane-amphibole rock (altered garnets-glaucophane eclogite).

The rock is porphyroblastic structure where Garnet grains are highly fragmented with wide cracks filled by quartz, epidote and amphibole. Some Garnet grains in size 3-4 mm are entirely replaced by quartz, chlorite, and zoisite aggregate, retaining only part of porphyroblasts. Garnet grains account for 10% of the rock. Base fabric is folded from randomly arranged grains of epidote of prismatic habit and short prisms of zoisite (40%), needled-diverse actinolite (30%), blue violet glaucophane (10%), green chlorite (15%), and quartz (5%). The grain size of epidote 0.4 - 0.8 mm, sometimes it forms aggregations of grains. There are fine-needled glaucophane and actinolite between grains of epidote. Patches of green chlorite flakes accumulation are presented. It is of a number of pennine, dark brown interference colors. The twinned plagioclase occurs along with quartz and chlorite. It is defined as the albite number 7 according to symmetrical extinction. The rock contains brownish granular grains of sphene size up to 0.1 mm.

The minimum regressive trend is in the range of 544-413 ºC/1.04 GPa and the progressive trend is in

the range 493-545 ºC/1,11 GPa corresponds to the 4th prograde cycle

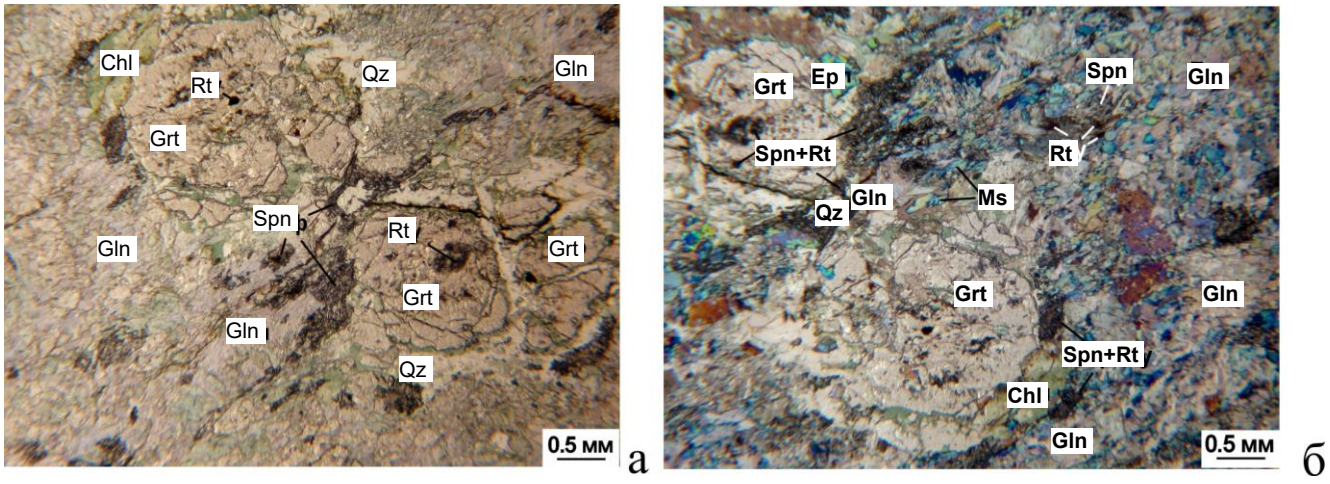


Fig. 14. Sample 230 (Novosimbirka area). The site near the village of Novosimbirka demonstrates the widest spread of P-T parameters at the exhumation stage of the Maksyutovsky complex: from the

highest prograde temperatures of Grt-Cpx equilibrium in sample 238-2-2 - 800-900 °C to the minimum regressive parameters among all the studied rocks - 545-310 °C with H = 1.0-1.2 GPa in Sample 230-B-1 (4th metamorphic cycle). Signs of prograde alterations in this named eclogite are still present in the same range of P-T values: T = 495-545 °C, P = 1.0-1.2 GPa (SM-2, Table 2). However, they are immediately inherited by the retrograde trend and are practically not preserved in this sample.

Ivanovka location

This site includes outcrops of altered eclogites in a small quarry on the outskirts of the village of Ivanovka. Initially, garnet-glaucophane eclogites underwent pre-temperature metamorphism at the level of the 2nd-3rd cycle in the range from T = 465-470 °C to 670-720 °C and P = 1.5-2.0 GPa (Samples 238-239). At the regressive stage of metamorphism, they successively transformed into Grt-Gln schists, and then into heavily altered rocks of the 3rd and 4th retrograde levels, repeating the same temperature range of prograde alterations: from 745-690 to 470-450 °C.

Thin section 288. Garnet-glaucophane schist.

The rock of porphyroblastic structure where garnet porphyroblasts have a round shape and filled by inclusions of minerals: quartz, glaucophane, epidote, chlorite, sphene and rutile. The poikilitic germination in garnet is twisted, indicating on tectonic effects on garnet grains. Grains of quartz and chlorite are developing along the edges of garnet grains. Base fabric is presented by grayish blue thin-needled of glaucophane and pale green needles of actinolite. Glaucophane and actinolite grains are elongated along the foliation. Between them there are lenses of quartz fine mosaic structure and stain accumulation of flakes of chlorite. Around of garnet porphyroblasts found muscovite, size up to 0.4 mm. Traces of pyroxene grains stored at main tissue between glaucophane needles. However, these grains are the entirely substituted by aggregate of epidote and chlorite.

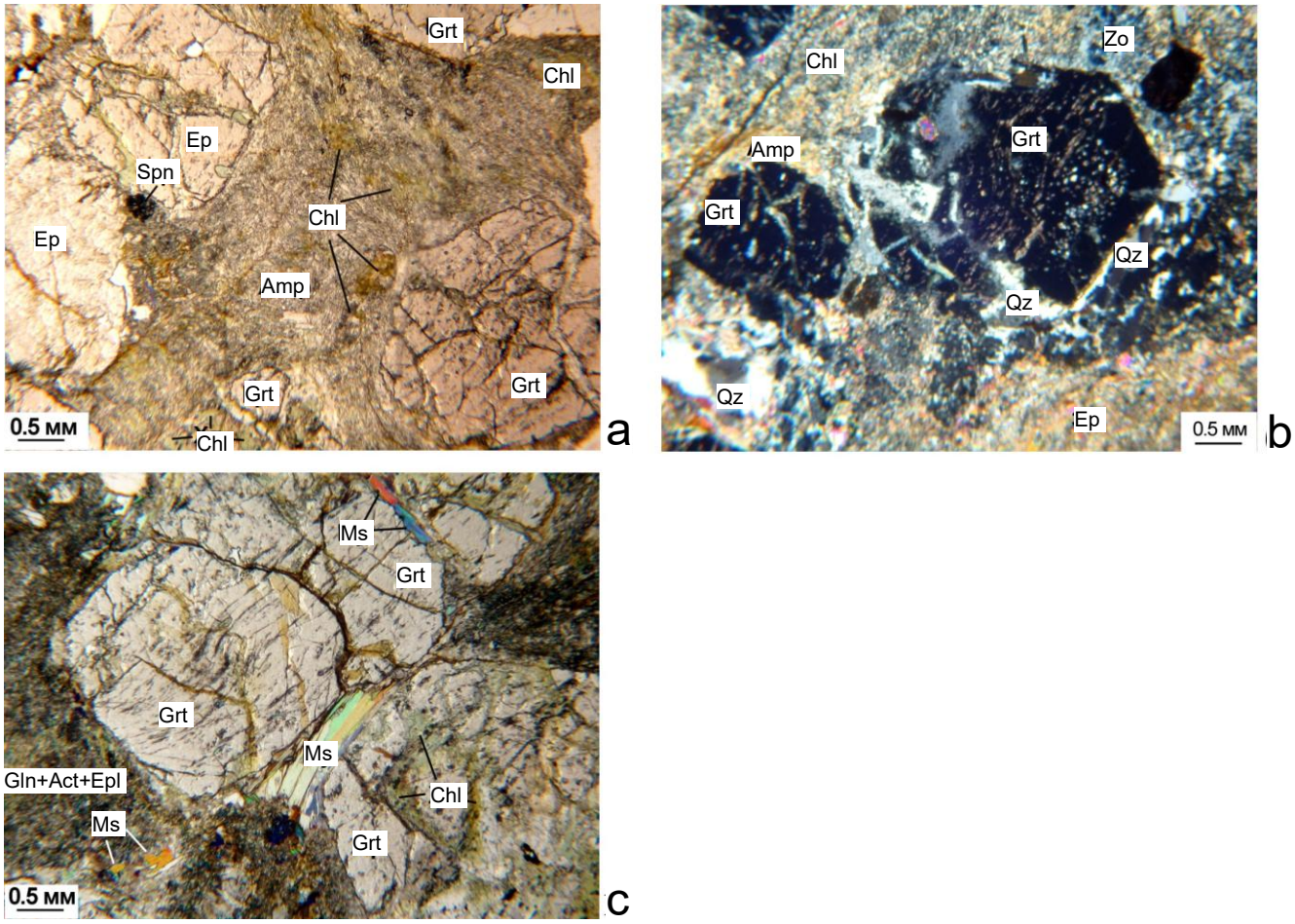


Fig. 15. Sample 288 (Ivanovka area), garnet retains distinct progressive zoning and, in equilibrium with pyroxene, displays a positive temperature trend from 460-485°C to 520-670°C. The compositions of four pyroxenes (Jd 36-38%) and Pl (0.64% An) are typical of the Karayanovo-Ivanovka eclogites. The pressure calculated using the Pl-Cpx-Qz barometer does not exceed 1.18-1.42 GPa and likely reflects the conditions of the final stages of metamorphism in the northern part of the Maksyutov complex.

Thin section 289-3-1. Garnet-epidote-actinolite-chlorite rocks (modified eclogite).

The rock of porphyroblastic structure where garnet porphyroblasts have shapeless appearance, are compressed and pilfered. Size garnet is from 0.5 mm to 4 mm. The following minerals are developed around garnet grains and along cracks: chlorite, muscovite, quartz, epidote, and sphene. Garnet porphyroblasts occupy up 20% of the rock volume. Base fabric rocks are finely scaly and fine needle unit of grains: green chlorite (30%), actinolite (10%), and yellowish grains of epidote (20%). All minerals have a direction along the schistosity. Within chlorite grains developing around garnet grains flakes of muscovite (5%) are found. They fuse with the chlorite. Quartz grains (5%) and plagioclase (albite) (5%) developed in the form of lenses and layers in the main fabric of rock. In addition to these minerals there is sphene (5%) in the rock. Sphene grains are small and have a spear-shaped form and developed in all the rock minerals.

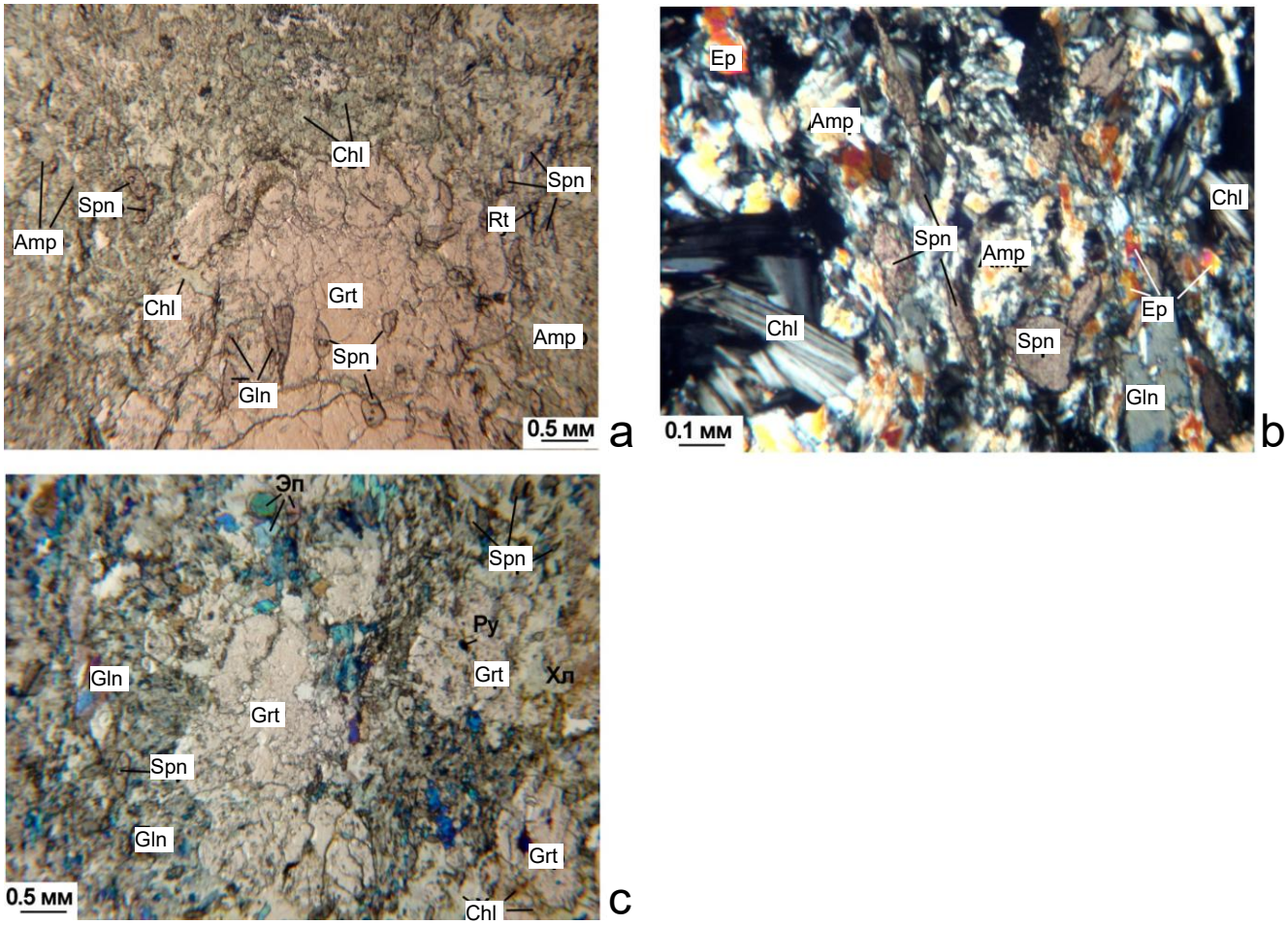


Fig. 16. Sample 289-3-1 (Ivanovka site) shows three progressive (in small grains) and three regressive (in large grains) trends (SM-2, Table 2). Large garnet grains in equilibrium with matrix clinopyroxene exhibit relatively high temperatures—up to 710-720°C. Newly formed small crystals and the edges of large grains exhibit lower temperatures—554-561°C.

Supplementary Files

This is a list of supplementary files associated with this preprint. Click to download.

- Table1.doc
- Supplementary1.doc
- Supplementary2Samplelist.doc
- Supplementary3SM3.doc
- Supplementary4.doc